Preparation of Novel, Nanocomposite Stannoxane–Based Organic–Inorganic Epoxy Polymers containing Ionic bonds

ARTICLE *in* MACROMOLECULES · JANUARY 2012

Impact Factor: 5.8 · DOI: 10.1021/ma201178j

Macromolecules

Article

pubs.acs.org/Macromolecules

Preparation of Novel, Nanocomposite Stannoxane-Based Organic–Inorganic Epoxy Polymers containing Ionic bonds

Adam Strachota,*[†] François Ribot,[‡,§] Libor Matějka,[†] Paul Whelan,[†] Larisa Starovoytova,[†] Josef Pleštil,[†] Miloš Steinhart,[†] Miroslav Šlouf,[†] Jiřina Hromádková,[†] Jana Kovářová,[†] Milena Špírková,[†] and Beata Strachota[†]

[†]Institute of Macromolecular Chemistry, Academy of Sciences of the Czech Republic, Heyrovskeho nam. 2, CZ-162 00 Praha, Czech Republic

[‡]UPMC, Chimie de la Matière Condensée de Paris (UMR 7574), Collège de France, 11 place Marcelin Berthelot, 75005 Paris, France

[§]CNRS, Chimie de la Matière Condensée de Paris (UMR 7574), Collège de France, 11 place Marcelin Berthelot, 75005 Paris, France

ABSTRACT: Polymer nanocomposites of epoxies with a novel filler, amino-functional butyltin oxide cage (stannoxane), were prepared and characterized. The nanofiller displays a promising antioxidizing effect, besides mechanical matrix reinforcement. The reinforcement can be assigned to physical interactions among the polymer bonded nanofiller. Moreover, the stannoxane cage undergoes a rearrangement to larger poly amino-functional nano-objects at higher temperatures, which highly reduces its extractability: it is practically not extractable from the nanocomposites in most cases. This, together with the fact that only a few weight percent are needed to achieve an optimal effect, makes it attractive as an antioxidative stabilizer. Epoxy–stannoxane nanocomposite synthesis, stannoxane reactivity and dispersion (morphology via TEM and SAXS), as well as the nanofiller effect on mechanical properties (DMTA) and on thermal stability are discussed. A brief comparison is drawn between the stannoxanes and the previously investigated POSS nanofiller.

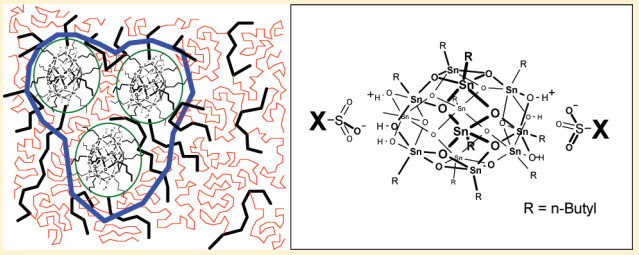

1. INTRODUCTION

Novel nanocomposite polymers were synthesized by the authors via reactive incorporation of butyl tin oxide cages (Scheme 1) into an epoxy matrix in order to achieve simultaneous mechanical reinforcement and antioxidative stabilization of the polymer. A general advantage of nanocomposites in comparison with classical ones consists in the small size of filler, which mostly makes possible the use of the same processing techniques for the nanocomposite, like for the neat polymer matrix[1−4] In case that the filler is sufficiently small in comparison to visible light wavelength, optical transparency is also preserved. Additionally, the intrinsic properties of the selected nanofiller can provide specific chemical,[5−7] optical,[8−10] electrical,[11−13] magnetic,[14−17] or gas barrier[18−21] properties to the final nanocomposite.

In their recent work, the authors investigated epoxy-nanocomposites reinforced by chemically bonded inorganic polyhedral oligomeric silsesquioxane (POSS) cages[22−24] and demonstrated the key importance of POSS–POSS interactions for the mechanical reinforcement in these nanocomposites. The organic substituents attached onto the POSS surface were shown to control the filler–filler interaction.[23] The physical cross-linking and the topological constraint to elastic chain motion caused by hard domains of aggregated (matrix-bonded) POSS nanofiller was demonstrated[24,25] to contribute to mechanical reinforcement as well as to increased thermal stability.

The ellipsoid shaped, 2 nm wide and 4 nm long[26] dodecameric butyl tin oxide ("stannoxane") cages shown in Scheme 1 are of similar size like POSS (with substituents typically 1.5 nm). The stannoxane cages are expected to possess interesting chemical properties, i.e. antioxidative ones, derived from tin chemistry. This attracted the authors' interest to epoxy-nanocomposites with the novel stannoxane filler. Only a few pioneering works were published up to date about polymeric materials containing stannoxane cages: Ribot et al. reported the preparation of carboxylate-based self-assembled organic–inorganic hybrids[27,28] with stannoxane and methacrylate–stannoxane copolymer.[29]

The attachment of two functional (or eventually inert) substituents by ionic bonds in axial positions of the stannoxane cage is a unique feature. The ionic bonding may cause interesting effects in stannoxane copolymers, especially concerning their eventual segmentation and mechanical behavior under stress. Ionic dissociation of the stannoxane end groups, anion exchange as well as supramolecular assembly under specific conditions were reported by Ribot et al.[30,31] It is

Received: May 24, 2011
Revised: November 24, 2011
Published: December 13, 2011

Scheme 1. Butylstannoxane Dodecamer Building Blocks $[(nC_4H_9{-}Sn)_{12}(O)_{14}(OH)_6][O_3S{-}X]_2$: (a) Chemical Structure of "Sn4", an Aromatic Diamine, and of "Sn_0" Non-Functional; (b) Symbolic Representation of Ionic Bonds in the Stannoxane Cages

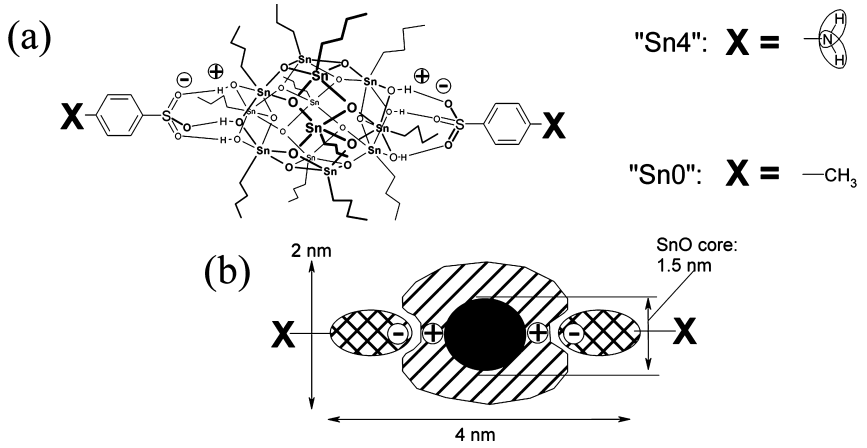

Scheme 2. Synthesis and Derivatization of the *n*-Butylstannoxane Dodecamer

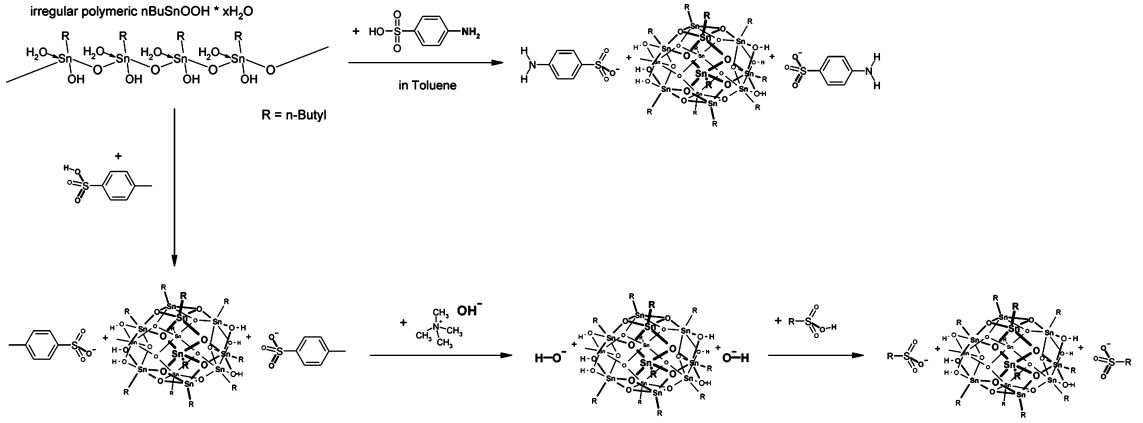

known,[32−35] that copolymers containing nonpolar main repeat units and small amounts of comonomer with an ionic side group (e.g., metal carboxylate or sulfonate), so-called ionomers, display valuable mechanical and melt properties. These result from association of the ionic-pair side groups to so-called multiplets (acting as reversible physical cross-links), small strong associates of up to eight ionic pairs. The ionic multiplets are able to aggregate to larger, looser, ion-rich domains (clusters), which contain also trapped nonpolar polymer segments. The nonpolar domains, ionic multiplets and multiplet clusters dominate the phase behavior of ionomers. In case of the studied stannoxane nano-objects, the effects of ionic bonding are expected to be weaker than in the above-mentioned ionomers, due to the fact that ionic bonding occurs between large neutral segments of the stannoxane, and that the ionic bonds are partly hidden, as illustrated symbolically in Scheme 1**b**, which is a strong difference to, e.g. sodium sulfonate side groups with "naked" metal cations. The ionic character of the bond to axial substituents is also likely moderated by hydrogen bridging, as marked by dotted bonds in Scheme 1a. The axial bifunctionality itself is a very valuable synthetic property of the stannoxane cages in comparison to most known nanofillers of similar size: e.g., POSS is typically obtainable in monofunctional or polyfunctional form. As a result of the bifunctionality, the stannoxanes can be easily incorporated into polymer backbones[27,28] or into other linear structures. In the present contribution, however, they are used as a four-functional reactant, with two two-functional "end-groups" in the axial positions.

Well-defined oligomeric alkylstannoxane cages similar to the one shown in Scheme 1 were first prepared in 1989 by Puff and Reuter,[36] followed by Dakternieks.[37] In some analogy to siloxane chemistry, a large family of stannoxane compounds exists,[38−40] including structures like linear, branched and ladder polymers, networks, drums and cages of different sizes. In 2000, Ribot,[26,41] one of the authors, developed a new, high-yield synthesis route (Scheme 2) to the butyl stannoxane dodecamer (Scheme 1), thus making possible the synthesis of large amounts and thorough product characterization. Ribot et al. also reported the cage's thermal lability[26] at temperatures above 250 °C.

Ribot's route to the stannoxane dodecamer (Scheme 2[26,41]) was used in this work, starting from the inexpensive butyltin oxide hydroxide polymer. The final product can be obtained in one step via reaction with the corresponding sulfonic acid, whose anions will form the axial functional substituents. In case that the acid is too weak, or does not support product crystallization, a longer (three-step) version of the synthesis is chosen (Scheme 2), via stannoxane dodecamer with toluenesulfonyl "end-groups", whose ionic substituents are subsequently exchanged for the strongly basic hydroxy anions. The latter ones are finally neutralized by the sulfonic acid to

dx.doi.org/10.1021/ma201178j | *Macromolecules* 2012, 45, 221−237

Scheme 3. Components and Idealized Structures of the Prepared Polymer Networks: (a) Diglycidyl Ether of Bisphenol A (DGEBA) and Phenyl Glycidyl Ether (PGE); (b) Poly(oxypropylene) α,ω-Diamine Jeffamine D2000, *n* = 33.6; (c) Symbolic Representation of the Stannoxane Nano-Building Blocks "Sn4" and "Sn_0"; (d) Explanation of Symbolic Building Block Representations used in Parts e–g; (e) Reference Network DGEBA–D2000[a]; (f) Network with "Sn4" Nano-Building Block Replacing Part of D2000[a]; (g) Network with Incorporated Non-Functional "Sn_0" Nano-Building Block

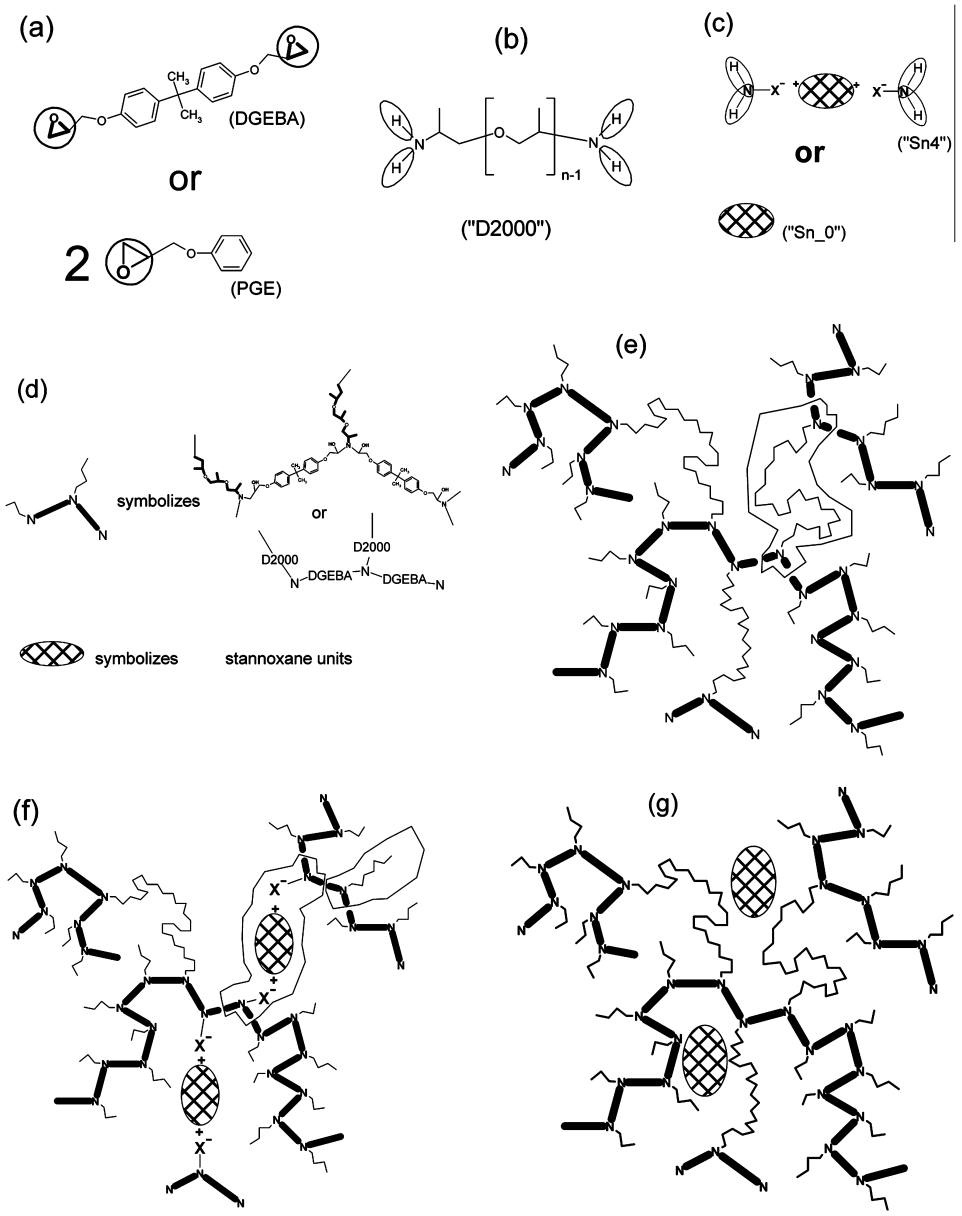

[a]In the images e and f, the components of the low molecular weight network model are encircled.

obtain the product with the desired functionality. The amino-functional stannoxane used in this work was prepared by the longer route, while the inert one in one step. Generally, a number of derivatives with different ionic end-groups can be prepared via the longer synthesis path, by neutralization of butylstannoxane dodecamer dihydroxide, e.g., compounds with carboxylate,[27,28] dialkylphosphinate,[30] or even sulfate[31] or oxalate[31] anions. Some anionic end groups could not be introduced up to date, however: This is especially the case of anions derived from aminoacids (amino-sulfonic, amino-carboxylic, etc.) whose zwitterionic state, as used for the neutralization step in the longer synthesis (Scheme 2), is too weakly acidic. In such cases, no neutralization (no end-group exchange) or only a partial one takes place. Highly "amino-reactive" amino–carboxylates or amino–sulfonates with primary aliphatic amino groups were not yet prepared for this reason. It was still possible to prepare an aminopropylsulfonate with a secondary, cyclohexyl-substituted aliphatic amino group using route of Ribot.[41] The reactivity of the latter product is reduced by sterical hindrance, however.

Previous studies of epoxy–POSS nanocomposites and the unique features of the newly available stannoxane cages inspired the investigation of novel epoxy-stannoxane nanocomposites. In order to achieve high sensitivity to mechanical reinforcement and to oxidative conditions, an elastomeric epoxy matrix was chosen, based on poly(oxypropylene)-α,ω-diamine (D2000)

dx.doi.org/10.1021/ma201178j | *Macromolecules* 2012, 45, 221–237

Table 1. List of the Prepared Polymers and Nanocomposites

sample name	mol % of Sn cage[a]	wt % of Sn cage	type of Sn cage	postcuring	fraction of gel w_g	w_g of filler	w_g of matrix
24-Sn_0	0	24.4	Sn_0	NO	0.89	0.64	0.97
24-Sn_0-pc	0	24.4	Sn_0	180 °C/12 h, under Ar	0.84	0.78	0.86
24-Sn_0-pcO	0	24.4	Sn_0	180 °C/12 h, in air	0.68	0.85	0.63
4-Sn4	4	4.1	Sn4	NO	0.97	0.98	0.97
4-Sn4-pc	4	4.1	Sn4	180 °C/12 h	0.88	0.99	0.88
10-Sn4	10	10.2	Sn4	NO	0.97	0.98	0.97
10-Sn4-pc	10	10.2	Sn4	180 °C/12 h	0.89	0.99	0.88
25-Sn4	25	24.4	Sn4	NO	1.00	1	1
25-Sn4-pc	25	24.4	Sn4	180 °C/12 h, under Ar	0.92	0.99	0.90
25-Sn4-pcO	25	24.4	Sn4	180 °C/12 h, in air	0.78	0.94	0.73
25-Sn4−240-Ar	25	24.4	Sn4	240 °C/30 min, under Ar	0.75	0.93	0.69
25-Sn4−240-O	25	24.4	Sn4	240 °C/30 min, in air	0.84	0.96	0.80
50-Sn4	50	45.5	Sn4	NO	0.97	0.98	0.96
50-Sn4-pc	50	45.5	Sn4	180 °C/12 h, under Ar	0. 93	1	0.87
50-Sn4-pcO	50	45.5	Sn4	180 °C/12 h, in air	0.91	0.98	0.85
100-Sn4[b]	100	80.3	Sn4	NO	x	x	x
DGEBA−D2000	0	0	no	NO	0.96	no	0.96
DGEBA−D2000-pc	0	0	no	180 °C/12 h, under Ar	0.85	no	0.85
DGEBA−D2000-pcO	0	0	no	180 °C/12 h, in air	0 (liquid)	no	0
DGEBA−D2000−240-Ar	0	0	no	240 °C/30 min, under Ar	0.72	no	0.72
DGEBA−D2000−240-O	0	0	no	240 °C/30 min, in air	0.61	no	0.61

[a]mol %("Sn4") = 100% * n(H(−N) stannoxane)/{n(H(−N) D2000) + n(H(−N) stannoxane)} where n is the chemical amount in mol. [b]The sample is too fragile for sol−gel analysis.

and diglycidylether of bisphenol A (DGEBA), see Scheme 3. The butylstannoxane nanofiller was expected to play two functions simultaneously: to reinforce the epoxy matrix mechanically, and at the same time to provide chemical stabilization similarly to tin based antioxidants. The stannoxane cages are covered by butyl groups, which—in analogy to similar POSS compounds—should lead to some solubility in the epoxy matrix, but also to a marked tendency to phase separation at medium and higher weight loads. As consequence, a relatively easy dispersion in the epoxy matrix should be achieved, while still preserving a considerable reinforcing effect by stannoxane-stannoxane interaction and aggregation. Of high interest was the effect of ionic attachment of the stannoxanes' functional substituents on thermomechanical properties, as well as the effect of high-temperature rearrangement of stannoxane cages.

2. EXPERIMENTAL PART

2.1. Materials. The poly(oxypropylene) diamines "Jeffamine D2000" (*molecular weight* = 1968 g/mol) and "Jeffamine D230" (*molecular weight* = 230 g/mol) were donated by Huntsman Inc. Diglycidyl ether of Bisphenol A ("DGEBA", 99.7% pure) was purchased from SYNPO a.s. Pardubice. Phenyl glycidyl ether (PGE) and 4,4′-diamino-diphenylsulfone ("DDS", IUPAC name: 4-[(4-aminophenyl)sulfonyl]phenylamine) were purchased from Sigma-Aldrich.

The amino-functional and the nonfunctional Stannoxane cages were synthesized as described earlier in the literature,[26,41] according to Scheme 2. Butyl tin oxide hydroxide hydrate, $BuSnO(OH).H_2O$, was used as starting material and reacted with toluenesulfonic or with sulfanilic acid to yield salts of the stannoxane cage dication shown in Scheme 2, "Sn_0" and "Sn4". The toluenesulfonate was converted into the dihydroxide in an ion exchange reaction using tetramethylammonium hydroxide. The dihydroxide was subsequently neutralized with sulfanilic acid, thus obtaining an improved yield of "Sn4". All above-mentioned chemicals were purchased from Sigma-Aldrich.

2.2. Nanocomposite Synthesis. The standard preparation method of epoxy-stannoxane nanocomposites was the so-called homogeneous procedure (homogeneous reaction mixture): The molten and supercooled epoxide DGEBA, the liquid Jeffamine D2000, and a 50 wt % stannoxane cage solution in toluene were mixed, the homogeneous clear reaction mixture was heated to 120 °C and stirred in an open vessel until gelation (typically ca. 40 min). Subsequently, the remaining solvent was removed by briefly applying vacuum at 120 °C. The plastic (and also clear, homogeneous) early postgel mixture was pressed into a mold (30 × 10 × 1 mm) and cured at 120 °C for 3 days. No air was entering the mold during the process.

For evaluation of the ability of the stannoxane to disperse via a reaction blending, so-called "heterogeneous" and "fine-heterogeneous" preparation procedures were also tested in addition to the homogeneous one. In the "fine-heterogeneous" synthesis the solvent (toluene) was removed at 25 °C under vacuum, just after mixing (stirring for 5 min) all components at room temperature. This led to microprecipitation of stannoxane (uniform crystals of around 5 μm size, as observed by optical microscopy), the precipitate having approximately a 100 times higher surface area in comparison to powdered "Sn4" stannoxane (grains of average width of 50 μm), hence the designation "fine-heterogeneous". The reaction mixture of milk-like color was poured into a mold (30 × 10 × 1 mm) and cured at 120 °C for 3 days.

In the case of the so-called "heterogeneous" preparation, neat powdered stannoxane (50 μm grains) was simply added to the other reaction components without any compatibilization. After thoroughly stirring the components at room temperature for 10 min, the opaque heterogeneous mixture was poured into a mold (30 × 10 × 1 mm) and cured at 120 °C for 3 days.

Postcuring of the prepared networks was achieved by heating the samples to 180 °C under argon atmosphere for 12 h.

"Oxidative post-curing" of the prepared networks was achieved by heating the samples to 180 °C in circulating air for 12 h.

The most important samples prepared are listed in Table 1. Only stoichiometric formulations were prepared, the stoichiometry being defined by the molar ratio of functional groups r = (amino-H)/(epoxy) = 1. The stannoxane ("Sn4") content in the formulations was quantified by the molar ratio of stannoxane amino-protons to all amino protons. This also corresponds to the molar percent of the organic diamine, "D2000", which was replaced by the equally diamino-functional stannoxane "Sn4" (both are four-functional in epoxy−amine additions). For example the abbreviation "25-Sn4" in Table 1 describes

dx.doi.org/10.1021/ma201178j | Macromolecules 2012, 45, 221−237

a polymer, in which 25 mol % of D2000 were replaced by "Sn4". In case of the nonfunctional nanofiller "Sn_0", its amount is given in wt %, e.g. "24-Sn_0". Special curing conditions are also part of the sample names, e.g. "25Sn4-pc" means additional 12-h postcuring at 180 °C under argon for the sample "25-Sn4".

2.3. Determination of the Gel Fraction. The sol−gel analysis of the network samples prepared was carried out as follows: The samples investigated were swollen and extracted with toluene/tetrahydrofuran (1:1). All the samples were extracted for 3 days while the solvent was changed every day for a pure charge. After the extraction, the samples were dried (vacuum, 100 °C) until weight constancy and the fraction of gel (w_g) was determined as

$$w_g = \text{mass (dry, after extraction)}/\text{mass (dry, before extraction)}$$

2.4. Determination of Stannoxane Content as SnO_2 Ash. The remaining stannoxane ("Sn4" or "Sn_0") content in the prepared nanocomposites after sol extraction was determined as SnO_2 ash mass. The analyses were performed as follows: The nanocomposite samples were put into a platinum pot together with the double of their weight of sulfuric acid. This mixture was slowly pyrolyzed in air (heating at around 337 °C, the boiling point of H_2SO_4). The remaining ash was heated to ca. 1000 °C for 15 min. The pyrolysis with the sulfuric acid was repeated once more with the ash. The dry SnO_2 ash was then weighed. From this result, the content on tin and on stannoxane (using the known weight fraction of tin in "Sn4" or "Sn_0") was calculated.

2.5. Dynamic-Mechanical Thermal Analysis (DMTA). Dynamic mechanical properties of the nanocomposite products were tested with rectangular platelet samples, using an ARES LS2 apparatus from Rheometric Scientific (now TA Instruments). An oscillatory shear deformation at the constant frequency of 1 Hz and at the heating rate of 3 °C/min was applied, and the temperature dependences of the storage shear modulus and of the loss factor (G' and tan(δ), respectively) were recorded. The temperature range was typically from −100 to +120 °C (or −100 to +100 °C in case of nanocomposites which were not postcured; in some cases the DMTA was recorded up to +150 °C). The geometry of the deformed area of all the tested samples was the same: 30 mm height, 10 mm width, and 1 mm thickness.

2.6. NMR Spectroscopy. Proton-decoupled ^{119}Sn solution NMR experiments were performed on a Bruker (Karlsruhe, Germany) Avance DPX 300 spectrometer at 111.92 MHz. The ^{119}Sn {^{1}H } spectra were obtained with a composite pulse decoupling sequence (CPD). $CDCl_3$ was used as solvent. The ^{119}Sn chemical shifts are quoted relatively to the tetramethyltin standard (δ = 0 ppm), in whose place the nonvolatile tetrabutyltin was used (δ = −7 ppm).

2.7. Small-Angle X-ray Scattering (SAXS). SAXS measurements were performed on a reconstructed Kratky kamera with a 60 μm entrance slit and a 42 cm sample-to-detector distance. Ni-filtered Cu Kα radiation (λ = 0.154 nm) was recorded with a linear position-sensitive detector (Joint Institute for Nuclear Research, Dubna, Russia). The experimental (smeared) SAXS curves are presented as a function of the magnitude of the scattering vector $q = (4\pi/\lambda) \sin \theta$ (2θ is the scattering angle).

2.8. Transmission Electron Microscopy (TEM). The TEM microscopy was performed with the microscope JEM 200CX (JEOL, Japan). TEM microphotographs were taken at the acceleration voltage of 100 kV, recorded on a photographic film, and digitized with a PC-controlled digital camera DXM1200 (Nikon, Japan). Ultrathin sections for TEM, approximately 50 nm thick, were cut with ultramicrotome Leica Ultracut UCT, equipped with cryo attachment.

2.9. Thermal Gravimetric Analysis (TGA). Mass-loss/temperature curves were obtained with a Perkin-Elmer TGA7 device. The samples were measured at a heating rate 10 °C/min. Nitrogen or air was used as a purge gas.

3. RESULTS AND DISCUSSION

The presented investigation of novel epoxy stannoxane nanocomposites is discussed in four chapters, dedicated to four interesting aspects of this work: the nanofiller dispersion in the epoxy matrix, the nanofiller's tendency to oligomerization and its consequences, the antioxidative effect of the nanofiller, and a brief comparison of the stannoxane nanofiller with the highly popular POSS nanofiller.

3.1. Dispersion of the Stannoxane Nanofiller in the Epoxy Matrix. In this chapter, topics related to nanofiller dispersion are discussed: the dispersion technique, the relative reactivity of the amino-functional nanofiller, sol−gel analysis of the prepared nanocomposites (filler extractability), the verification of the dispersion via TEM and the effect of the nanofiller dispersion on the mechanical properties.

The amino-bifunctional butylstannoxane dodecamer "Sn4" (size: 2 × 2 × 4 nm,[26] structure: Scheme 1), was successfully dispersed in the DGEBA−D2000 epoxy matrix, which was proven by transmission electron microscopy (TEM, see below: Figure 2 and section 3.1.3). The cage-like "Sn4" compound is only moderately soluble in the mixture of the matrix components, DGEBA and D2000, even at the cure temperature of 120 °C. The cure temperature and duration were chosen in analogy to previous work on inorganic nanocomposites with the same matrix.[22−24] The study of compatibilization and subsequent reactive incorporation of "Sn4" was of key importance. For this purpose, a homogeneous (solvent present until gelation), a finely heterogeneous (microsuspension; solvent present only during mixing) and a heterogeneous (suspension; without any solvent) preparation procedures were tested for the composition "25-Sn4". The morphology analyses, and even the mechanical properties (DMTA) of the nanocomposites showed, that only the solvent-assisted homogeneous preparation led to a good dispersion of the stannoxane nanobuilding blocks (comparison of Figure 2, parts a and b). This preparation was selected as standard procedure. In case of the heterogeneous and fine heterogeneous preparation, considerable filler incorporation was nevertheless achieved (see DMTA in Figure 4). This suggests, that reaction blending might be successful at small weight loads of "Sn4". However, for reasons of good comparability, all samples, even such with small "Sn4" content were prepared by the homogeneous procedure, using toluene as solvent.

A more advanced, solvent-free synthesis might be of interest for eventual larger-scale production of the nanocomposites, especially of such with low "Sn4" content: the reaction of excess DGEBA with "Sn4" in presence of solvent, followed by solvent removal, and the use of the DGEBA−Sn4(DGEBA)$_4$ mixture as epoxy component, eventually after addition of further DGEBA, in order to achieve the desired "Sn4" content. This synthesis was also tested, namely for the DGEBA/"Sn4" ratio of 8/1 (critical theoretical ratio for gelation would be 6/1). In place of a soluble mixture of epoxides, an insoluble polymer network with relatively good mechanical properties was obtained. The result indicated, that a careful optimalization of this synthesis route would be necessary, especially in order to prevent epoxy group homopolymerization. Consequently, the "DGEBA-capping route" was abandoned in this work, while it is still being further developed, especially for further improvement of antioxidative properties. The most important of the prepared samples are listed in Table 1, including their abbreviations, compositions and cure conditions.

dx.doi.org/10.1021/ma201178j | Macromolecules 2012, 45, 221−237

3.1.1. Relative Reactivity of the "Sn4" Nanofiller. The reactivity of the amino-functional stannoxane cages plays an important role in the morphology formation of the stannoxane−epoxy nanocomposites (Scheme 3). The same reactivity of amino groups of nanofiller ("Sn4") and of the organic amine (D2000) would favor a good dispersion of "Sn4" in the matrix. In contrast, a distinctly higher or lower "Sn4" reactivity would favor its preferential incorporation in early or late stages of the polymer formation, respectively, which in both cases would result in microphase separation and formation of "Sn4"-rich domains.

Using the same experimental technique like in previous work,[24] the relative reactivity of amino groups of "Sn4", of poly(oxypropylene)-α,ω-diamine ("Jeffamine D230", model for D2000) and of 4,4′-diaminodiphenylsulfone ("DDS", model for end-groups of "Sn4") were compared: The amines were reacted with excess phenyl glycidyl ether (PGE) at same stoichiometric ratios, concentrations and temperature, and the consumption of epoxy groups was measured via ^{1}H NMR, using the characteristic signal of the oxirane ring at 2.81 ppm (>CH- proton). The consumption of amino groups was assumed to be equal to the consumption of epoxy groups, thus assuming only negligible homopolymerization of PGE at the rather moderate reaction temperature of 120 °C. The reactivity comparison is shown in Figure 1. The half times of the reaction are as follows:

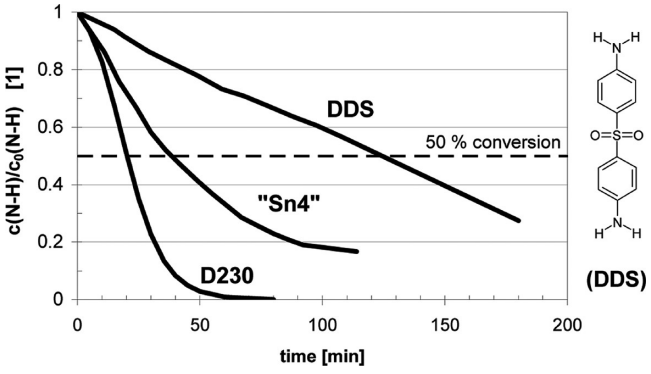

Figure 1. Relative reactivity: kinetic curves of consumption of N−H functionalities of the diamines "Sn4", DDS and of Jeffamine D230, in reaction with excess phenylglycidyl ether, T = 120 °C, in sealed ampule, r(H(−N)/Ep) = 0.25, c_0(Ep) = 3.48 M, c_0(Am) = 0.85 M, in toluene, determined via epoxy group conversion.

125 min for DDS, 39 min for "Sn4" and 20 min for Jeffamine D230. The nanofiller "Sn4" is markedly less reactive than the amino component of the matrix because "Sn4" is an aromatic primary amine, while Jeffamines D are aliphatic primary amines. "Sn4" is hence incorporated preferentially only in the later stages of the polymer synthesis, which together with the limited solubility in the matrix favors its aggregation to "Sn4"-rich domains.

Interesting is the much higher reactivity of the "Sn4" aromatic diamine in comparison with the model compound DDS. This finding suggests a catalytic role of the stannoxane cage, probably of its OH groups. The stannoxane catalytic effect with respect to the epoxy-amine addition was proven by gelation experiments with "Sn4" and also with its nonfunctional counterpart "Sn_0": The time of gelation (reaction samples in sealed ampules, visual observation of solidification with the precision of ±1 min) of the neat DGEBA−D2000 system at 120 °C is 70 min, while the system "25-Sn4" (fine heterogeneous preparation) gels already in 48 min. Similarly, the system DGEBA−D2000−24 wt %Sn_0 ("24-Sn_0") also gels faster: in 51 min, despite the moderate dilution of the system by the nonfunctional "Sn_0" cage. The "Sn4" stannoxane cages hence speed-up the formation of the DGEBA−D2000 network, and in spite of the lower reactivity of their own amino groups they probably also achieve at least an incomplete covalent attachment to the polymer matrix (see Sol−Gel Analysis discussion just below) in late reaction stages, due to the mentioned catalytic effect.

3.1.2. Sol−Gel Analysis: Study of Nanofiller Extraction. The extraction of the eventual unbound stannoxane nanofiller from the epoxy nanocomposites was tested using a 1:1 toluene/tetrahydrofuran mixture, in which both nanofillers "Sn4" and "Sn_0" are highly soluble (up to ca. 65 wt %), and which also easily swells the DGEBA−D2000 matrix. The results are summarized in Table 1. Given the lower reactivity and late incorporation of stannoxane "Sn4" into the epoxy matrix, a microphase separation of some unbound "Sn4" domains would be expected, especially at a high "Sn4" loading, in analogy to similar POSS systems.[24] An increased "Sn4"-rich sol fraction should be the result. However, it was determined that "Sn4"-containing nanocomposites show very small sol fractions, even smaller than the neat epoxy matrix. Moreover, a low sol fraction was found even in the nanocomposites with the inert, nonfunctional "Sn_0" filler, which should be extractable as it does not form bonds to the matrix. In the case of the sample "24-Sn_0" (24 wt % of "Sn_0") the achieved gel fraction was 89%, indicating that more than the half of the chemically unbound "Sn_0" filler was not extracted. This result is explained by the stannoxane cage tendency to rearrange to larger (nonextractable) polymers under the synthesis conditions. The ^{119}Sn NMR analysis (see further below, chapter 3.2) proved that 18% of the stannoxane cages polymerize (more exactly oligomerize) during the standard-applied cure at 120 °C for 3 days under argon. The polymerized stannoxane fraction (larger structures, which only difficultly can disentangle from the epoxy network) is the likely reason for the low extractability of nonfunctional "Sn_0", as well as of eventual unbound "Sn4". Furthermore, the above discussed catalytic effect of the stannoxane on the epoxy-amine reaction leads necessarily to a high conversion of the organic matrix and to a decreased fraction of the sol. This same catalytic effect also increases the likeliness of bonding of the less reactive "Sn4" diamine to the matrix by at least one bond (out of four possible).

Interesting results are obtained if the fractions of gel are determined for matrix alone and for nanofiller alone (in addition to the overall gel fraction, see Table 1). The stannoxane gel fractions are always relatively high, in most cases close to 1, and markedly higher than gel fractions of the cyclopentyl−POSS−DGEBA nanofiller which was investigated in a similar bonding situation in previous work[24] (w_g(POSS) was in the range 0.49−0.66). The partial gel fractions of the matrix in the nanocomposites are also slightly higher or identical like in the case of the neat DGEBA−D2000 matrix (Table 1), as far as the compared samples were cured at 120 °C.

3.1.3. Nanofiller Aggregation Study by TEM. The degree of nanofiller dispersion or eventual aggregation in the epoxy-stannoxane nanocomposites was assessed by means of transmission electron microscopy (TEM). The homogeneously prepared (toluene present until gel point) epoxy-"Sn4"

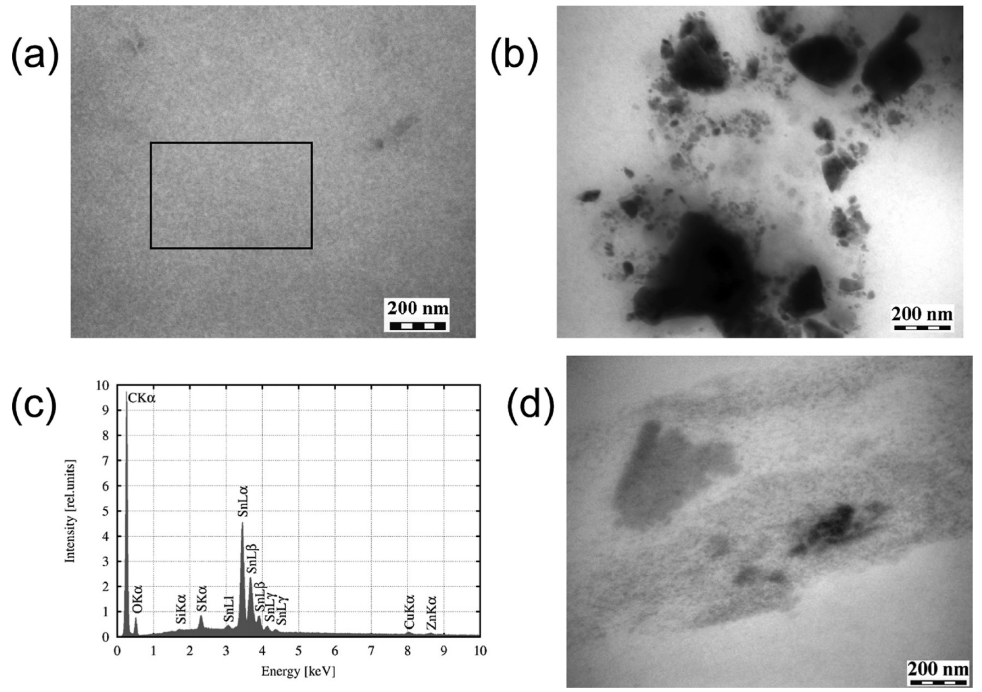

Figure 2. TEM micrographs of nanocomposites: (a) "50-Sn4"; (b) "25-Sn4-fine-heterogeneous preparation"; (c) EDXS analysis of "50-Sn4" (image a) 600 × 400 nm area; (d) "24-Sn_0".

nanocomposites (even with 50 mol % "Sn4") display a very fine nanofiller dispersion (Figure 2a), homogeneous up to the 10 nm scale. Somewhat smaller heterogeneities can be observed in the micrograph. The elemental EDXS analysis (Figure 2c) proves the presence of Sn from stannoxane in the nearly homogeneous nanocomposite the morphology of which is shown in Figure 2a. Fine heterogeneous sample preparation (solvent present only during mixing) leads to imperfect dispersion with numerous large stannoxane domains (dark), sized typically between 50 and 400 nm, as shown in Figure 2b. In contrast to the "Sn4" nanocomposites, the ones with the nonfunctional "Sn_0" nanofiller are always highly heterogeneous (Figure 2d), because the nonfunctional "Sn_0" can not undergo reaction blending and is only moderately soluble (like "Sn4") in the epoxy matrix if no solvent is present. Hence, independently of the preparation technique, "Sn_0" precipitates in later matrix formation stages. "Sn_0" domains of varying size, up to hundreds of nanometers can be seen in Figure 2d. Large "Sn_0" crystallites (sized ca. 2000 × 400 nm) can also be observed (not depicted).

3.1.4. Effect of the Dispersed Nanofiller on Thermomechanical Properties. The incorporation of the "Sn4" nanofiller markedly influences the thermomechanical properties of the DGEBA−D2000 matrix. Figure 3 shows the temperature dependence of the shear storage modulus G' and of the loss factor $\tan(\delta)$ of DGEBA−D2000−Sn4 polymers with 0−100 mol % "Sn4". Until 10 mol % of "Sn4", the nanofiller effect is moderate, but clearly visible, particularly by increasing T_g values (shift of $\tan(\delta)$ maxima). The content of 25 mol % or more of "Sn4" leads to distinctly different DMTA profiles.

Figure 4 illustrates the effect of nanofiller dispersion technique on the thermomechanical properties: A small increase of reinforcement can be seen if comparing the DMTA profiles of samples prepared by the "heterogeneous" and "fine heterogeneous" techniques, respectively. The reinforcing effect of "Sn4" markedly increases, if the sample is prepared by the homogeneous technique, using toluene as solvent.

The somewhat complex glass transition behavior of the DGEBA−D2000−Sn4 nanocomposites can be explained by taking into account the miscibility of phases in this copolymer: The DGEBA−D2000 matrix is a copolymer of two fully miscible phases (see structure in Scheme 3**e**). The more rigid phase consists of DGEBA units connected through nitrogen atoms ("−DGEBA−N−DGEBA−N− chains"; N originates from amino groups which underwent addition to the epoxy end-groups of DGEBA). This rigid phase alone displays a glass transition (T_g) around +70 °C. The second phase of the matrix consists of flexible elastic D2000 chains (poly(propylene oxide), T_g around −70 °C). The D2000 chains interconnect the DGEBA−N−DGEBA−N− chains at every N atom. The described copolymer displays a uniform glass transition near −29 °C, which is a result of the full miscibility of its phases.

The $\tan(\delta) = f(T)$ graphs of the nanocomposites in Figure 3 display profiles typical of copolymers with immiscible phases. It is possible to assign three main thermal transitions: the glass transition of the unhindered DGEBA−D2000 copolymer around −30 °C (predominantly movements of the flexible D2000 chains), the glass transition of DGEBA−D2000 immobilized by the sterical constraint of closely neighboring hard nanofiller domains in the region from −15 to +15 °C, and the glass transition assigned to the stannoxane-rich copolymer domains which shifts from +30 °C to +70 °C. The latter domains contain the DGEBA−Sn4 copolymer and some included D2000 chains. The transition is likely due to the loosening of larger secondary aggregates (see Scheme 4) composed of primary strong ones (composition: DGEBA−Sn4), between which some immobilized matrix (composition DGEBA−D2000) is included. The secondary "Sn4" aggregates are expected to be few and weak (more intercalated) at low "Sn4" contents, but stronger at high contents, with average distances between primary and also between secondary

dx.doi.org/10.1021/ma201178j | *Macromolecules* 2012, 45, 221−237

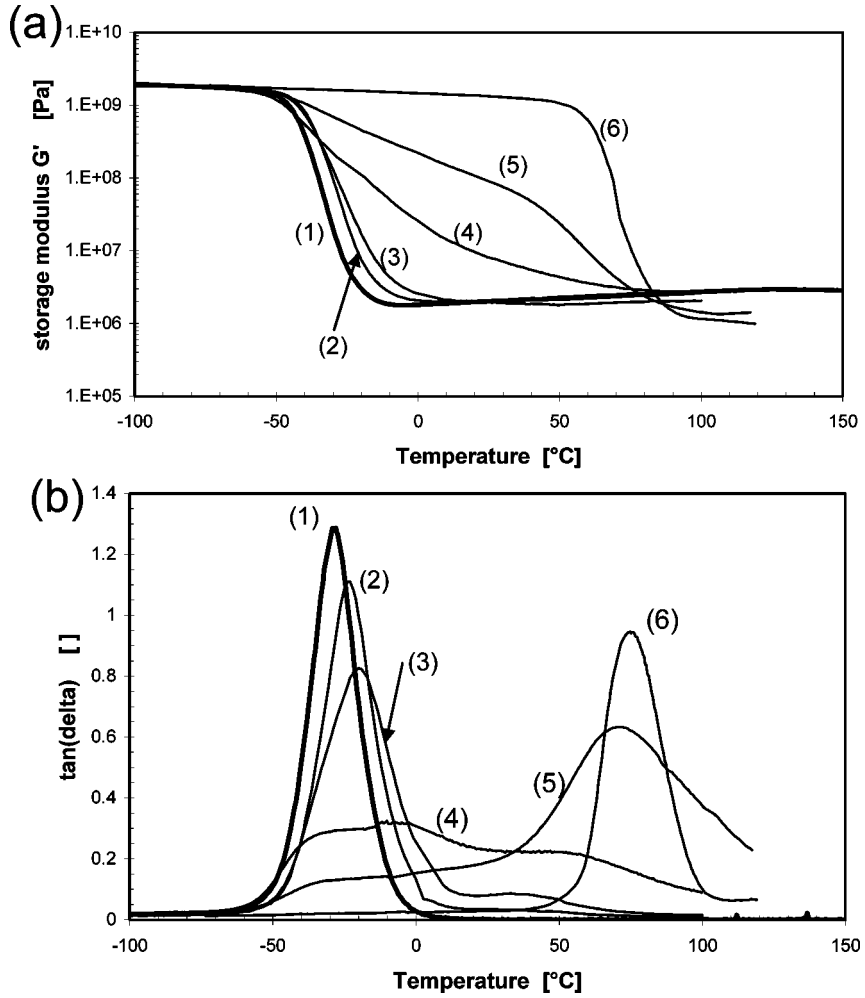

Figure 3. Shear storage modulus G' (a) and loss factor $\tan(\delta)$ (b) as a function of temperature: Effect of increasing content of the stannoxane "Sn4" on the mechanical properties of the epoxy nanocomposites: (1) DGEBA−D2000 reference; (2) 4 mol % D2000 replaced with "Sn4"; (3) 10 mol % "Sn4"; (4) 25 mol % (24 wt %) "Sn4; (5) 50 mol % "Sn4"; (6) 100 mol % "Sn4".

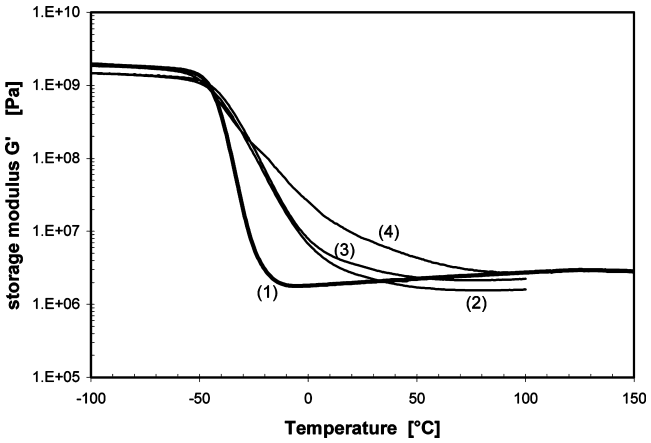

Figure 4. Effect of dispersion technique in samples cured at 120 °C: (1) neat DGEBA−D2000 matrix, (2) heterogeneous preparation of 25 mol % Sn4, (3) "fine heterogeneous", (4) homogeneous.

aggregates becoming short. Finally, at 100 mol % of "Sn4", only one phase, the DGEBA−Sn4 copolymer, is present in the sample, with all "Sn4" units in close contact, which leads to the highest T_g of the "stannoxane-rich phase". For comparison, the melting of neat "Sn4" occurs at a much higher temperature, 253 °C, followed by rapid polymerization. The presented interpretation is supported by the behavior of analogous samples, which underwent the polymerization (more exactly oligomerization) of the "Sn4" cages in the stannoxane domains (see further below, chapter 3.2). The proposed nanofiller arrangement is somewhat similar to the one observed in the so-called ionomer polymers,[32−35] which was mentioned in the introduction.

The contents of the different phases in the nanocomposites are illustrated by the $\tan(\delta) = f(T)$ graphs (Figure 3b): With increasing "Sn4" content, the peak of the free DGEBA−D2000 rapidly decreases and broadens and the peak of the immobilized DGEBA−D2000 adds to the first. The peak of the stannoxane-rich-phase's glass transition grows, shifts to higher temperatures and becomes narrower. For compositions with very small or very high nanofiller content, sharp transitions are observed indicating rather uniform systems. At low "Sn4" contents, especially at 4 mol % the behavior is close to a system with all phases miscible (copolymer effect of rigid "Sn4"), while at higher "Sn4" loadings the behavior of immiscible phases prevails, in parallel to the observed solubility of "Sn4" in the matrix.

The epoxy networks with high "Sn4" content show smaller rubbery moduli than the neat matrix after the relaxation of the

dx.doi.org/10.1021/ma201178j | *Macromolecules* 2012, 45, 221−237

Scheme 4. Thermal Rearrangement of Aggregated Butylstannoxane Cages to Larger Structures, Which Keep the Ionic-Bonded Functional Substituents[a]

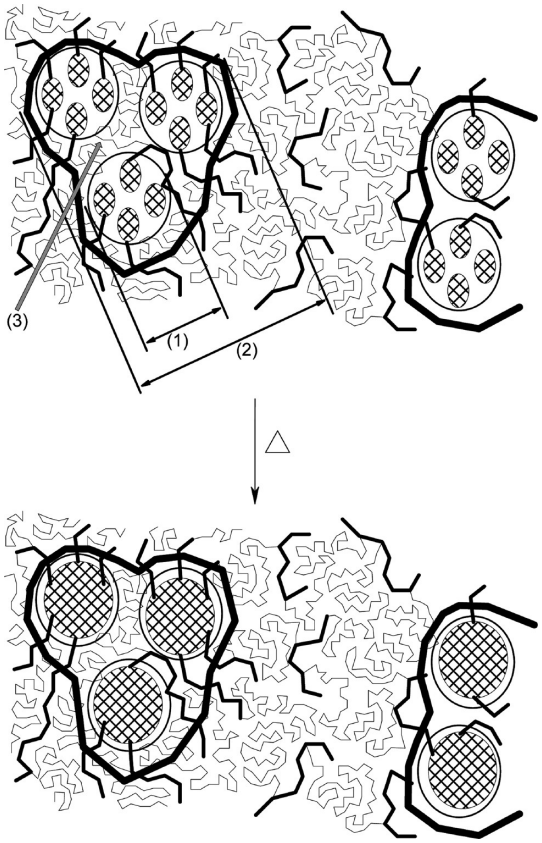

[a] Explanation: (1) = primary "Sn4" aggregates; (2) = secondary "Sn4" aggregates; (3) = matrix chains inclusions in the secondary aggregates.

reinforcing structures at high T, obviously due to incomplete conversion of "Sn4" amino goups and the resulting lower cross-linking density.

3.2. Rearrangement of the Stannoxane Cages to Larger Structures. An interesting property of the "Sn4"-epoxy nanocomposites is the oligomerization of "Sn4" inside of its domains, which was found to occur during the nanocomposites postcure at elevated temperatures. The "Sn4" polymerization and its effects on material properties were studied exemplarily for the nanocomposite with 25 mol % "Sn4" by means of SAXS, TEM, ^{119}Sn−NMR, and DMTA. On the other hand, attempts to easily detect the "Sn4" polymerization by means of differential scanning calorimetry (DSC) failed, probably due to approximate thermo-neutrality of the process. Melting closely followed by rapid polymerization at 253 °C can be observed on a thermostated plate, if a neat "Sn4" sample is put on it near this temperature, and if the heating rate is fast.

Nanocomposite was investigated in order to increase the degree of chemical incorporation of the less reactive aromatic-amino-functional stannoxane into the epoxy polymer. For this purpose, samples were annealed at 180 °C for 12 h, under argon atmosphere (in order to prevent oxidative side-reactions). The temperature program was chosen on the base of previous experience with epoxy-nanocomposite synthesis[22−24] and with reactivity of aromatic amines toward epoxides.[42] At the chosen postcure temperature, however, a partial rearrangement of "Sn4" aggregates to larger structures (Scheme 4) was suspected,[26] as well as some thermal degradation of the matrix (see Table 1, gel fraction of the neat matrix after postcure). The rearrangement of "Sn4" was indeed proven as discussed below, and was found to be a prominent process during the postcure at 180 °C, and even to occur to a small extent at 120 °C. Because of a complex nanocomposite morphology (Scheme 4), only an oligomerization of "Sn4" is possible, and additionally, this process does not affect significantly the thermomechanical properties of the nanocomposites, but may help to reduce the stannoxane extractability. The "Sn4" polymerization to larger cages probably involves a reversible dissociation of the ionic bonds to the functional substituents, as proposed in Scheme 5. This would be in analogy to the known finding,[38,26] that protonation/deprotonation reactions play a key role in the synthesis and reorganization of different stannoxane structures.

3.2.1. Stannoxane Cage Polymerization Studied by SAXS and TEM. The study of "Sn4" cages polymerization via a temperature-dependent SAXS experiment is illustrated in Figure 5a: A specimen of the "25-Sn4" nanocomposite was gradually heated to 240 °C and subsequently cooled to room temperature, while SAXS patterns were recorded, all under argon atmosphere.

The SAXS patterns of the DGEBA−D2000−Sn4 nanocomposites cured at 120 °C can be assigned as follows: The scattering intensities show a distinct interference maximum near q = 0.42 Å^{-1}, which characterizes the size of a single "Sn4" stannoxane cage, more exactly its highly dense inorganic tin−oxo core (1.5 nm). This interference maximum was found not to shift with changing "Sn4" content (from 4 to 100 mol %, see Figure 5b) and hence corresponds to an internal distance inside the "Sn4" cage. A marked increase of scattering intensity followed by a plateau is observed in the region q = 0.1 to 0.05 Å^{-1} and can be fitted using the Guinier function for spherical particles. This pattern can be assigned to X-ray scattering on larger heterogeneities − aggregates of "Sn4" building blocks, sized typically around 11 nm. Such an aggregate size was found for 25 and 50 mol % "Sn4", while with 10 mol % the aggregate size was smaller: 6−7 nm (at 4 mol % "Sn4": too weak scattering from aggregates).

Upon annealing the "25-Sn4" sample (Figure 5a) little change occurs in the SAXS patterns, until the temperature increases above 220 °C. Above this temperature the patterns

Scheme 5. Postulated Mechanism of the Dissociation/Reconnection of the Ionic Bond to the Functional Substituent, via Deprotonation/Protonation of a Bridging Oxygen Atom (Analogy to, e.g., Ammonium and Phosphonium Salts)

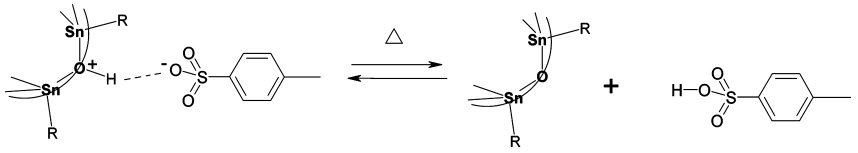

dx.doi.org/10.1021/ma201178j | Macromolecules 2012, 45, 221−237

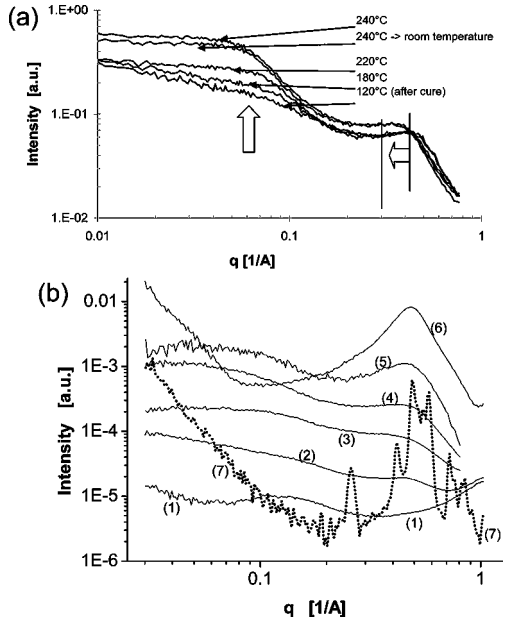

Figure 5. (a) SAXS investigation of stannoxane polymerization in the nanocomposite "25-Sn4": heating from 30 to 240 °C at 5 °C/min, followed by cooling at the same rate. (b) SAXS patterns of the nanocomposites prepared. Effect of Sn4 filler amount: (1) = 0 mol % (neat matrix), (2) = nanocomposite with 4 mol % Sn4, (3) 10 mol % Sn4, (4) 25 mol % Sn4, (5) 50 mol % Sn4, (6) 100 mol % Sn4, and (7) neat Sn4 (dotted).

markedly change, and the profile finally observed at 240 °C does not change any more after the sample is cooled back to room temperature. The annealing causes a shift of the "Sn4-width-interference" maximum to lower q values (Figure 5a), around 0.32 $Å^{-1}$, corresponding to an increased size of the inorganic cage cores (1.9 nm). At the same time, the slope and the plateau intensity in the small-angle region increase. This indicates changes in the stannoxane aggregates: The slope increase suggests their increasing compactness. Furthermore, the Guinier analysis of the small-angles region indicates that the stannoxane domains also decrease in size from 11 to 5 nm. The SAXS observations allow in combination with the above-discussed DMTA results the following interpretation: Before annealing, the (2 nm wide) "Sn4" building blocks form strong and small primary aggregates containing only a few units, sized around 3 nm (interpenetration of the butyl substituents). The primary aggregates are loosely assembled to secondary aggregates (Scheme 4) sized around 11 nm and intercalated with matrix. Upon heating above 220 °C, the "Sn4" units in the primary aggregates quickly polymerize to larger compact blocks which extend over the whole primary aggregates. The original large and loose secondary domains differentiate into several smaller and denser regions in which a few primary domains are more compactly arranged. These smaller aggregates are then separated by wider matrix intercalations and become distinguishable by means of SAXS.

In order to evaluate the changes of stannoxane domain size by an additional independent method, TEM images of an exemplary sample (50 mol % "Sn4") annealed under argon at 180 and at 240 °C were acquired. No visible difference of domain morphology was observed in comparison with the micrograph taken prior to annealing (Figure 2a). This means that in spite of the above observed "fracturing" of the secondary domains to smaller units, the latter ones remain arranged to similar patterns like before the annealing.

3.2.2. Polymerization of the Stannoxane Cage Studied via ^{119}Sn NMR. The polymerization of the stannoxane nanobuilding blocks under standard preparation conditions and at elevated temperatures (postcuring) was studied quantitatively using ^{119}Sn NMR. Solid-state NMR spectra of both neat stannoxane[26] and of the epoxy-stannoxane nanocomposite (not depicted) consist of complex signals and are hence difficult to compare and evaluate unequivocally. On the other hand, the liquid ^{119}Sn NMR spectrum of the stannoxane cage is very simple: 2 singlets corresponding to 2 types of Sn atoms in the structure (see Figure 6a). For this reason, a liquid low-molecular-weight model (see Scheme 3) of the nanocomposite with 25 mol % "Sn4" (DGEBA−D2000−Sn4) was synthesized, possessing also the same reactivity of the components: Monofunctional phenyl glycidyl ether (PGE) was used as the epoxy component in place of bifunctional DGEBA. The soluble PGE−D2000−Sn4 model made it possible to measure liquid ^{119}Sn NMR spectra of the stannoxane after the epoxide-amine addition at 120 °C, and after subsequent heating (postcuring) at elevated temperatures. In this way the stannoxane polymerization at different conditions was determined quantitatively using an internal integration standard (tetrabutyltin added just prior to NMR analysis). The Figure 6 compares the spectra of the low molecular weight model PGE−D2000−Sn4 just after component mixing at room temperature (Figure 6a), after cure at 120 °C for 3 days (Figure 6), after cure at 120 °C and subsequent postcure under Ar at 180 °C for 12 h (Figure 6c), and after cure and subsequent postcure at 240 °C for 30 min under Ar (Figure 6d). The signal of the integration standard (nBu$_4$Sn) can be seen at −7 ppm, while the stannoxane cage signals appear at −273 ppm (five-coordinated Sn atoms in "equatorial region" of the cage) and −453 ppm (six-coordinated Sn atoms in "polar regions"). The rearranged (polymerized) stannoxane does not display (as reported in ref 26) any new Sn NMR signals, probably due to signal broadening given by irregular structures and possibly also due to long relaxation times of the tin atoms in the large polymeric stannoxane structures.[26] The results in Figure 6 show, that the stannoxane building blocks mainly survive (82% unchanged, 18% polymerized) the cure at 120 °C. A relatively large part survives also the postcuring at 180 °C under argon (44%). The tin signals of the surviving cages become broader, probably due to an increased amount of chemical defects in their close surrounding. The short (30 min) heating to 240 °C leads to the complete disappearance of the two stannoxane dodecamer signals, indicating a complete rearrangement of all stannoxane cages to polymer. The results are in good correlation with the temperature dependent SAXS profiles discussed above.

3.2.3. Effect of Stannoxane Polymerization on Thermomechanical Properties. Interestingly, the polymerization of the "Sn4" nanofiller building blocks was found not to cause any marked change in the thermomechanical properties (DMTA profiles in Figure 7) of the standard homogeneously prepared DGEBA−D2000−Sn4 nanocomposites. The DMTA profiles of the nanocomposites postcured under argon at 180 °C for 12 h are nearly the same like DMTA profiles after the standard cure at 120 °C for 3 days, which are shown in the comparison in Figure 7 further below. Only small differences were observed: the tan(δ) values for the postcured samples were always slightly lower, and the tan(δ) peaks assigned to the loosening of the secondary stannoxane aggregates (glass transition of the

dx.doi.org/10.1021/ma201178j | *Macromolecules* 2012, 45, 221−237

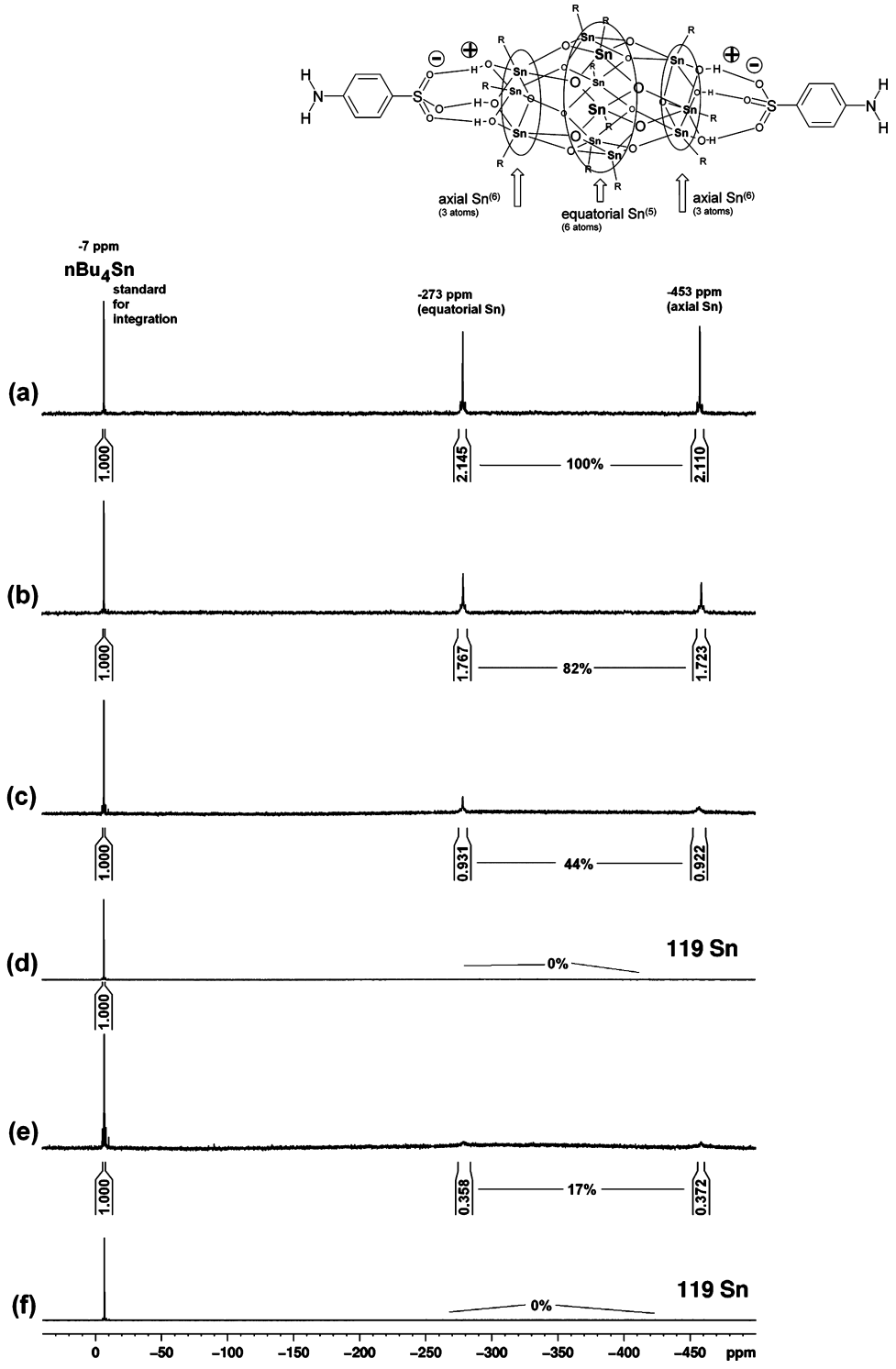

Figure 6. ^{119}Sn NMR spectra: (a) of the PGE−D2000−Sn4 mixture containing 25 mol % of amino groups from "Sn4", after mixing at room temperature (low molecular weight model of the nanocomposite with 25 mol % "Sn4"); (b) low molecular weight model after 3-days-cure at 120 °C under argon; (c) additionally postcured for 12 h at 180 °C under argon; (d) additionally postcured for 30 min at 240 °C under Ar; (e) additionally oxidatively postcured for 12 h at 180 °C under air; (f) additionally postcured for 30 min at 240 °C under air.

stannoxane-rich phase) were shifted to moderately higher temperatures. Both effects could have been caused by the polymerized primary stannoxane domains being more rigid (and more compactly arranged) than the nonpolymerized ones and causing a more efficient immobilization of the epoxy chains.

Brief postcuring at 240 °C (30 min under argon, DMTA not depicted in Figure 7 because of strong overlaps) has a nearly identical effect on the mechanical properties like postcuring at 180 °C, but the rubbery moduli are lower, indicating that the thermal matrix degradation is no longer negligible. The postcure at 240 °C was tested in order to obtain samples

dx.doi.org/10.1021/ma201178j | *Macromolecules* 2012, 45, 221−237

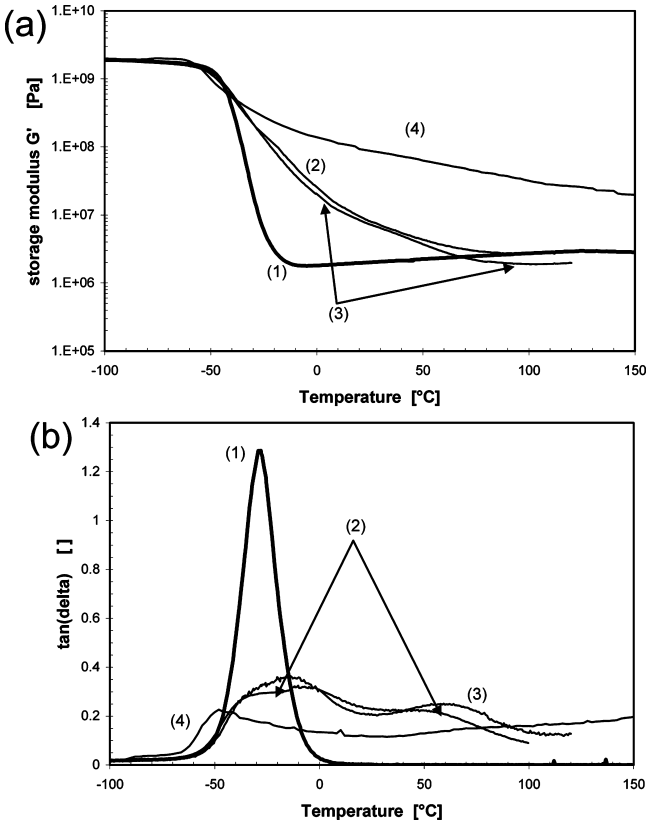

Figure 7. Effect of cure conditions on the thermomechanical properties of the "25-Sn4" nanocomposite, Shear storage modulus G' (a) and loss factor tan(δ) (b) as a function of temperature: (1) neat DGEBA–D2000 matrix cured at 120 °C; (2) "25-Sn4" nanocomposite cured at 120 °C; (3) "25-Sn4" additionally postcured for 12 h under argon; (4) "25-Sn4" additionally postcured for 12 h in air.

with completely polymerized stannoxane nanofiller (postcure at 180 °C/12 h leads only to 56 % of "Sn4" being polymerized).

3.2.4. Sol–Gel Analysis after Stannoxane Polymerization. The samples postcured under argon at 180 °C for 12 h, and especially at 240 °C for 30 min, display higher sol fractions, especially for the matrix component, (Table 1) than the standard (120 °C) cured ones. This is obviously due to the thermal degradation of the DGEBA–D2000 matrix, as observed via DMTA (see above). An analogous degradation can be also observed for the neat matrix.

3.3. Antioxidative Stabilizing Effect of the Stannoxane. A very attractive property of the stannoxane nanofiller consists in its behavior as an antioxidative stabilizing agent in the studied epoxy matrix. The effect was studied via sol–gel and thermogravimetric analysis, and also via DMTA. The mechanism of the stabilization was verified by means of ^{119}Sn NMR, ^{1}H NMR (using liquid low molecular weight analogues), through comparative tests with the "Sn_0" filler and by study of viscosity changes in liquid nanocomposite anologues. The antioxidative effect of the "Sn4" nanofiller manifests itself very strongly in the mechanical properties (DMTA). The tests of oxidative degradation of mechanical properties were performed by exposing the samples to the temperature of 180 °C in circulating air, for 12 h, while the neat matrix DGEBA–D2000 degrades to a brown liquid in half this time (in 6 h) under these conditions. Except for the exposition to air, the oxidative postcure conditions were the same like in case of the nonoxidative postcure under argon. A strong antioxidative effect of-"Sn4" is observed in the sol–gel analysis of oxidized samples, while the TGA results alone did not show any marked effect. "Sn4" hence achieves a strong stabilization, without at the same time preventing small mass losses.

3.3.1. Sol–Gel Analysis. The stannoxane nanobuilding blocks strongly hinder the oxidtaive fragmentation of the epoxy matrix, as can be seen from comparison of gel fraction of "oxidative post-cured" (12 h/180 °C/air) samples (Table 1). The neat matrix degrades quantitatively to a brown liquid mixture (gel fraction falls to 0%). In the "Sn4" nanocomposites the gel fraction falls to values between 80 and 70%, depending on the stannoxane content. While the oxidative degradation is not prevented completely, the stabilization is still fairly successful from the point of view of sol–gel analysis. The brief oxidative postcure at 240 °C leads to a smaller drop in the gel fraction then the prolonged one at 180 °C. It has to be taken into account, that the oxidative postcure at 240 °C for 30 min makes possible a complete oligomerization of "Sn4" (only about 1 min is needed for this process at 240 °C), but the oxidative degradation is a slower process: approximately 2 h would be needed for the degradation of the neat matrix, as determined by visual observation.

3.3.2. Thermogravimetric Analysis (TGA). The results of thermogravimetric stability investigations of epoxy–stannoxane nanocomposites are illustrated in Figure 8. Only TGA traces in

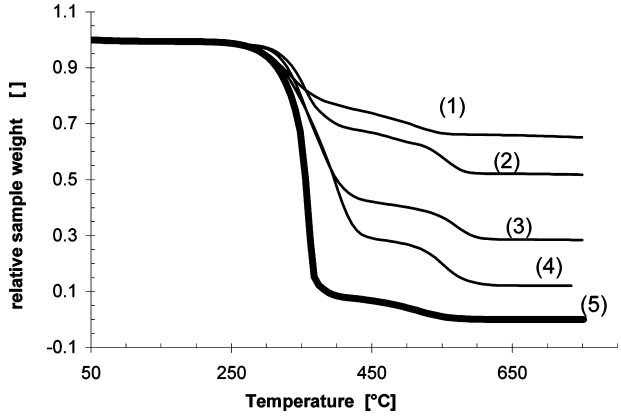

Figure 8. TGA traces in air: relative sample weight in dependence of the temperature (at 10 °C/min): (1) neat "Sn4" stannoxane; (2) epoxy–stannoxane nanocomposite cured at 120 °C containing 100 mol % "Sn4"; (3) 50 mol % "Sn4"; (4) 25 mol % "Sn4"; (5) DGEBA–D2000 reference.

air are shown. From the thermogravimetric point of view, the stannoxane "Sn4" in most cases does not stabilize the nanocomposites against mass loss upon oxidative heating. This is in contrast to the observed stabilization of mechanical properties against their oxidative degradation, as discussed below. "Sn4" itself displays a slightly smaller stability in air and in nitrogen than the neat matrix DGEBA–D2000. This means that "Sn4" starts to significantly react with oxygen somewhat earlier than the matrix, which also might explain its tendency to oxidative cross-linking reactions with the matrix, which are discussed just below. Still, some nanocomposites display moderately improved TGA stability in air, e.g., the one with 50 wt % "Sn4". Normally cured, postcured, and oxidatively postcured samples display very similar TGA profiles.

3.3.3. Antioxidative Stabilization Observed via DMTA. Epoxy–"Sn4" nanocomposites postcured in air at 180 °C for 12

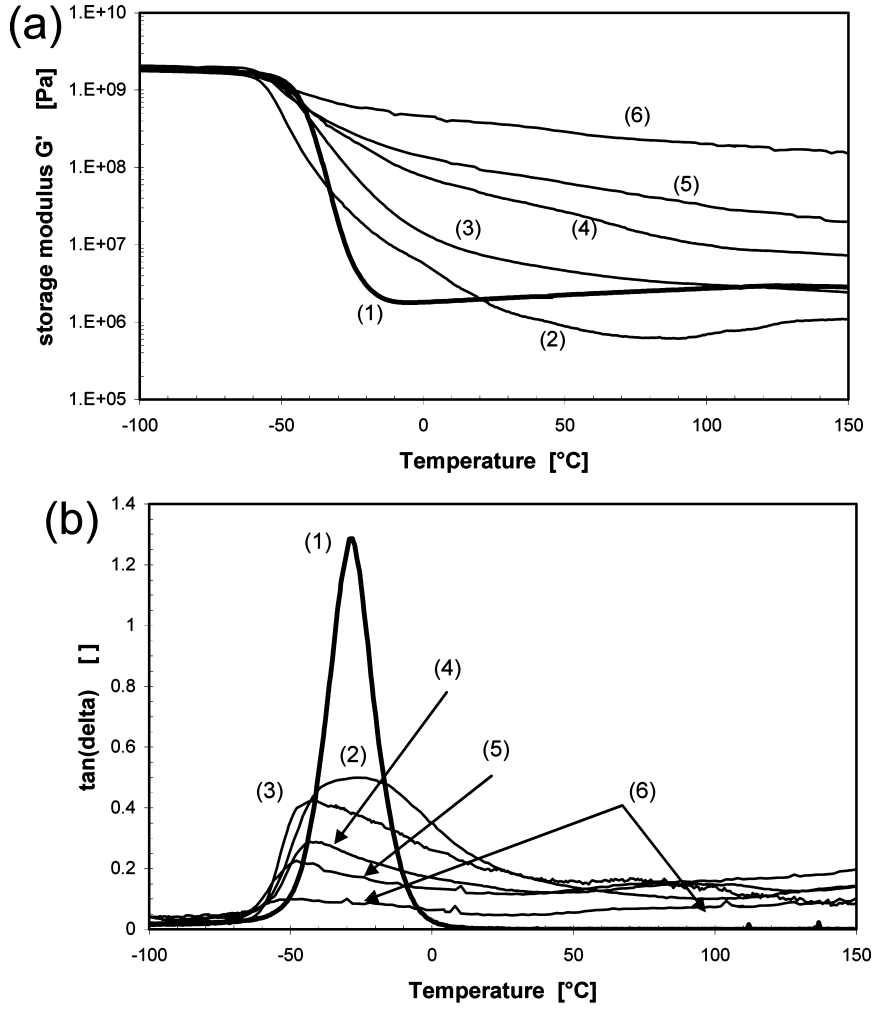

Figure 9. Shear storage modulus G' (a) and loss factor tan(δ) (b) as a function of temperature. Effect of oxidative postcure: (1) reference network DGEBA–D2000 cured at 120 °C; epoxy-"Sn4" nanocomposites after oxidative postcure in air at 180 °C for 12 h; (2) composite with 4 mol % "Sn4", (3) with 7%, (4) with 10%, (5) with 25%, and (6) with 50%.

h, display a dramatically increased rubber modulus after this treatment, especially if the stannoxane content is high, see Figure 9. In contrast to this, the reference sample, DGEBA–D2000, degrades to a brown liquid during this postcure.

The $G' = f(T)$ profiles indicate an increase in cross-link density: Markedly higher equilibrium rubber moduli are observed in comparison to the neat matrix. The effect of mechanical reinforcement via "oxidative post-curing" increases very strongly with increasing "Sn4" content (Figure 9). The amount of 7 mol % (corresponding approximately to 7 wt %) of "Sn4" seems to be optimal to prevent oxidative degradation of mechanical properties under the given treatment (12 h/180 °C/air) and to keep a good material toughness at the same time. Smaller nanofiller amounts are no more sufficient for stabilization, while high stannoxane contents lead not only to strong modulus increase but also to fragility (small deformation at break: only about 1% for "S0-Sn4-pcO") after the oxidative treatment. The tan(δ) = $f(T)$ profiles of the oxidatively postcured samples differ strongly from profiles of analogous samples cured at 120 °C (Ar) or postcured at 180 °C under argon. An increase of T_g and a broadening of the transition region of the stannoxane-rich phase is observed, indicating larger structures with stronger mutual interactions. The transitions of the neat matrix are also broadened, due to some amount of oxidative damage.

3.3.4. Explanation of the Antioxidative Effect. The presumed mechanism of the antioxidative action of "Sn4" is most likely based on radical cross-linking reactions between the stannoxane and the matrix as suggested in Scheme 6. Such reactions are expected to lead to additional covalent matrix-stannoxane and stannoxane-stannoxane bonds, and thus to an increased chemical cross-link density. This effect counteracts and overrides the cross-link density decrease caused by oxidative matrix degradation, and leads to the observed rubber moduli increase and to the preservation of a relatively high fraction of gel, see Table 1. The behavior of the liquid low molecular weight models of the nanocomposites (used for NMR experiments) is a further evidence of the oxidative cross-linking reactions: Upon postcuring in air at 180 °C, the complex viscosity of the liquid model increases strongly (from 5 to 65 Pa·s), while after the 240 °C postcure in air, the liquid model becomes a rubbery gel, and can be only partly dissolved. Analogous postcuring under argon leads to no marked viscosity increase (from 5 to 6 Pa·s).

The effects of oxidative cross-linking were also followed via ^{119}Sn NMR (Figure 6e,f): Only 17% of the original dodecameric stannoxane cages survive after the oxidative

dx.doi.org/10.1021/ma201178j | *Macromolecules* 2012, 45, 221–237

Scheme 6. Possible Oxidative Radical Cross-Linking Reactions Involving: (a) Stannoxane and the Epoxy Matrix; (b) Two Stannoxane Cages

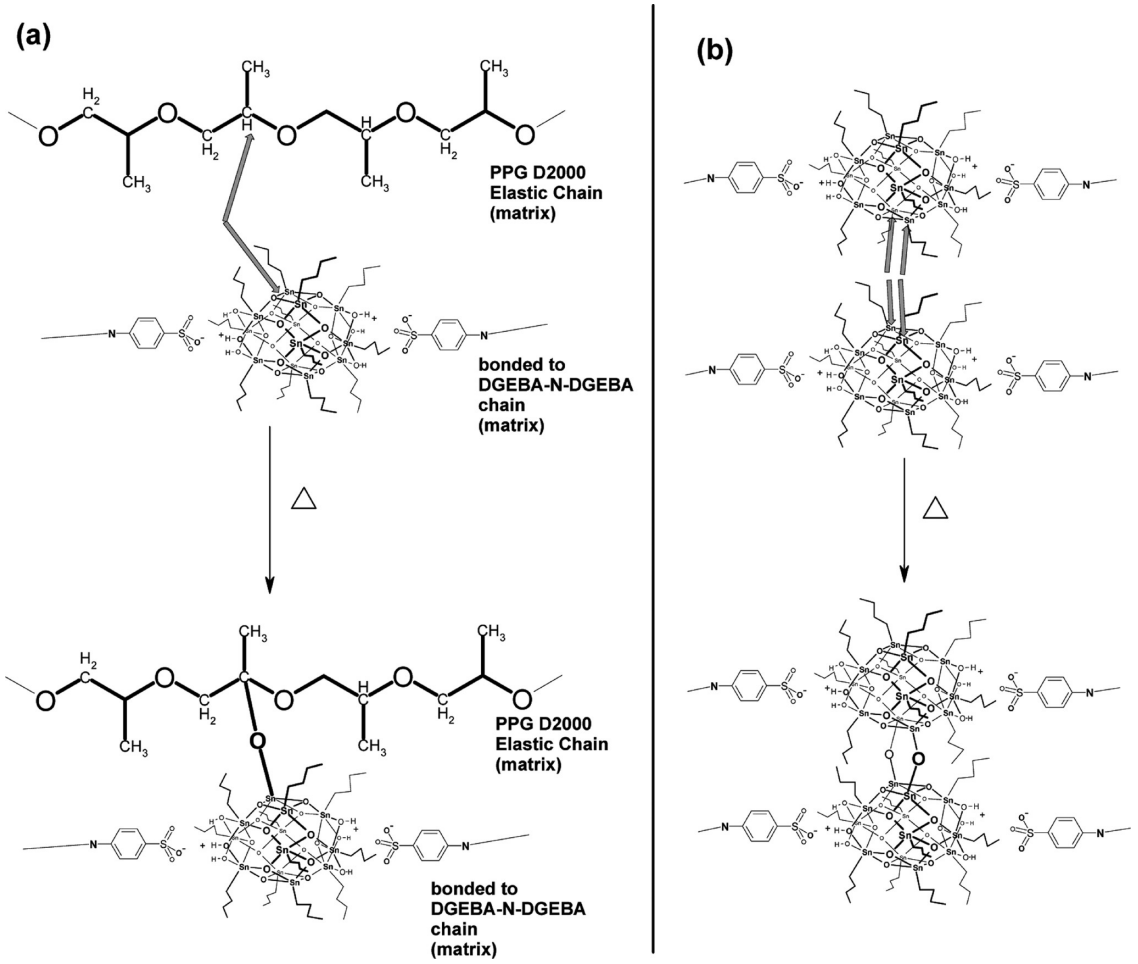

postcure at 180 °C (12 h), while under argon, 44% survived an analogous postcure. The missing 27% are presumedly the stannoxane units which were linked to the D2000 (Scheme 6a) molecules or with each other (Scheme 6b) by radical cross-linking. A further confirmation of the oxidative radical cross-linking was sought via ^{1}H NMR spectroscopy (Figure 10) using also the liquid model: An oxidative radical reaction involving the break of the Sn−C bonds (butyl groups) would lead to the decrease of the butyl groups signals in the spectra of the oxidatively postcured samples. Reactions involving the ionic bonded functional substituents of the stannoxane would lead to the change or disappearance of their aromatic signals. Indeed, a strong decrease of the integrals of stannoxane butyl groups (relative to D2000 "matrix" signals) is observed in Figure 10. The signals of the aromatic functional groups seem also to undergo some change, meaning that these groups do not stay intact, but their intensity is too small for a reliable evaluation.

In search of a more direct proof for stannoxane bonding to the matrix via oxidative cross-linking, the nanocomposite with the nonfunctional stannoxane "Sn_0" (24 wt %) was investigated under postcure and oxidative postcure conditions. "Sn_0" does not reinforce the DGEBA−D2000 matrix; neither does it do so after cure at 120 °C, or after subsequent 180 °C postcuring under argon, as demonstrated by DMTA profiles in Figure 11. However, after oxidative postcuring (12 h/180 °C/air), the DMTA profile changes (Figure 11 curve 4) to a shape similar like in case of the nanocomposite containing 25 mol % of chemically bonded "Sn4" (Figure 3 curve 4), with a typical broad transition region caused by mutual interactions of matrix bonded stannoxanes. This directly proves the chemical attachment of the previously unbonded stannoxane "Sn_0" to the epoxy matrix, as a result of the oxidative postcure. From the application point of view it can be seen, that the "Sn_0" filler is much less an efficient stabilizer then "Sn4" (comparison of the oxidative postcuring of "24-Sn_0" and of "25-Sn4"). This is a result of the strong microphase separation of "Sn_0" in the nanocomposites with DGEBA−D2000, which leads to large "Sn_0" domains (TEM, see above, Figure 2d) with a small specific surface.

3.4. Brief Comparison of Stannoxane vs POSS. In view of the authors' recent research about POSS−epoxy nanocomposites,[22−25] it is interesting to compare the effect of silsesquioxane (POSS) and stannoxane ("Sn4") cage-like nanofillers. If similar amounts of "Sn4" (which replaces D2000) and of the strongly reinforcing cyclopentyl−POSS−DGEBA (which replaces DGEBA) are incorporated into the DGEBA−D2000 matrix, e.g., around 25 wt %, then the mechanical reinforcing effects in the rubber region are of comparable strength for both fillers, while marked differences are also obvious, as illustrated in Figure 12. In case of nanocomposites cured at 120 °C under air exclusion, "Sn4" is rather a weaker reinforcing agent than Cp−POSS−DGEBA:

dx.doi.org/10.1021/ma201178j | *Macromolecules* 2012, 45, 221−237

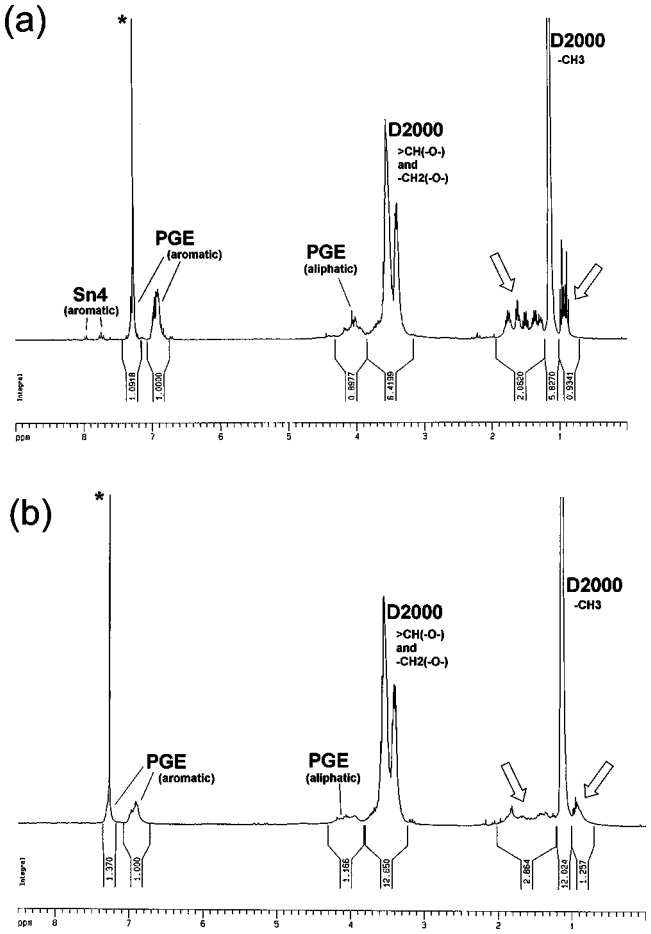

Figure 10. ^{1}H NMR spectra of the low molecular weight model of "25-Sn4" (PGE–D2000–Sn4): (a) after cure at 120 °C for 3 days under argon; (b) after subsequent oxidative postcure at 180 °C in air for 12 h. Signals of butyl substituents of "Sn4" are marked with arrows.

Stronger reinforcement by "Sn4" is only observed between −30 °C and +20 °C, while at higher temperatures Cp–POSS–DGEBA reinforces much stronger. On the other hand, in case of samples treated by oxidative postcure, the stannoxane causes a stronger reinforcement than POSS (cured at 120 °C, postcured or oxidatively postcured) in the complete temperature range.

A typical feature of the stannoxane-filled nanocomposites is the continuous decrease of the reinforcing effect with temperature. On the other hand, reinforcement with POSS leads to a "lifted" plateau of shear modulus in the rubber region, followed by a relatively steep step in modulus around 130 °C, where the most of the reinforcing POSS structures relax. As already discussed above, several thermal transitions are observed in the stannoxane-epoxy nanocomposites, (free matrix, matrix hindered by sterical constraint, and "Sn4"-rich phase), adding together to form a broad transition region. Especially broad is the transition of the "Sn4"-rich phase: the strong primary stannoxane (matrix-bonded "Sn4") aggregates are associated with looser, matrix intercalated secondary ones, which display a wide range of stabilities. In contrast to this, Cp–POSS–DGEBA at 25 wt % reinforces by small primary aggregates (of matrix-bonded POSS), which all possess rather similar stability and disconnect in a narrow temperature range. (Only at very high Cp–POSS–DGEBA loads are effects like matrix immobilization observed.)

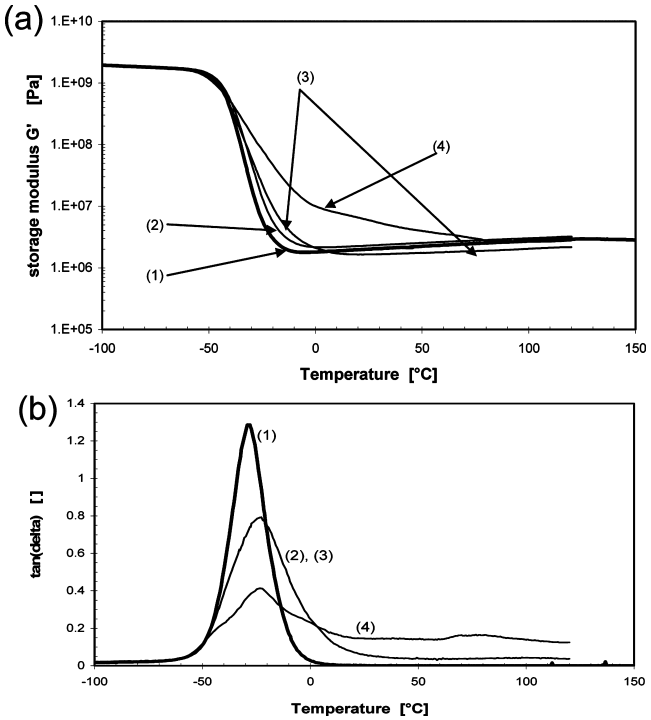

Figure 11. Shear storage modulus G' (a) and loss factor tan(δ) (b) as a function of temperature. Effect of inert nanofiller "Sn_0" on mechanical properties (DMTA profiles) depending on curing and postcuring conditions: (1) DGEBA–D2000 reference (120 °C); (2) network with 24 wt % "Sn_0" cured at 120 °C; (3) "24-Sn_0" postcured (180 °C) under argon; (4) 24 wt % "Sn_0" oxidatively postcured in air (180 °C).

A unique and attractive feature of the stannoxane, which was not yet found for POSS, is its ability of stabilizing epoxies against oxidative degradation of mechanical properties via radical cross-linking reactions. Such behavior was not observed in nanocomposites with POSS. Cp–POSS–DGEBA can still slow down the oxidative degradation (probably by hindering oxygen diffusion) in comparison to the neat matrix as illustrated in Figure 12: while the neat matrix degrades to a liquid after the applied oxidative postcure, the Cp–POSS–DGEBA reinforced nanocomposite displays a decrease of the modulus in the rubber region by one order, but still remains a soft solid. Postcure under argon at 180 °C also leads to a small but significant degradation of the POSS-reinforced sample (Figure 12). However, under more drastic conditions, like treatment with atomic oxygen (low earth orbit conditions)[43,44] or under irradiation with hard UV light[45] (which is able to photochemically fragment the matrix), POSS was observed to protect nanocomposites via formation of a protectiove SiO_2 layer, which is an attractive feature.

4. CONCLUSIONS

Novel hybrid organic–inorganic epoxy networks containing butylstannoxane dodecamer nanobuilding blocks, with two ionic-bonded amino-functional substituents, were successfully prepared. The addition of toluene as solvent was necessary in order to disperse the nanofiller homogeneously.

Nanometer-scaled phase separation nevertheless occurs in the later stages of the nanocomposite syntheses, because the nanofiller solubility in the matrix is only moderate. This

dx.doi.org/10.1021/ma201178j | Macromolecules 2012, 45, 221–237

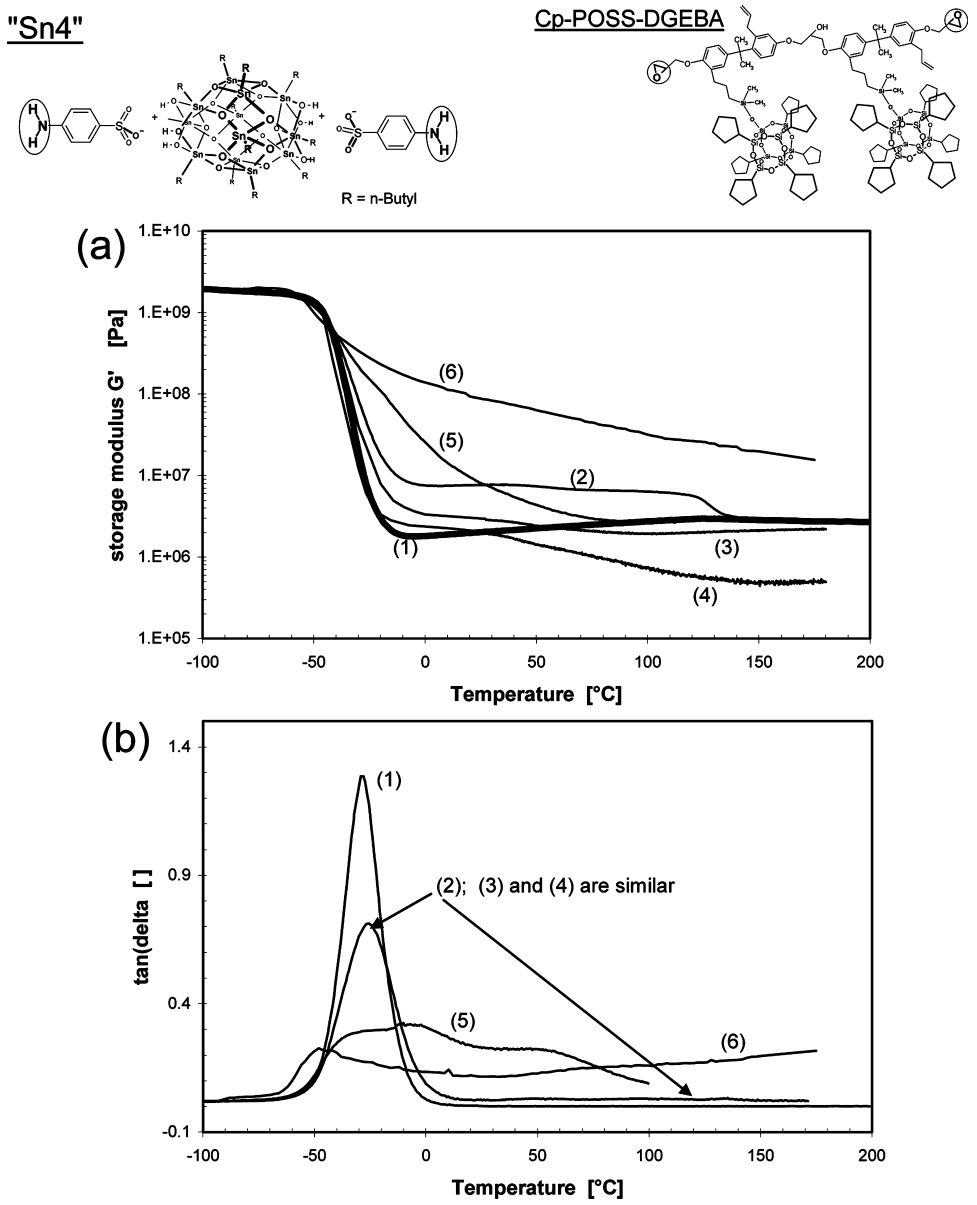

Figure 12. Comparison of stannoxane "Sn4" and of the strongly reinforcing cyclopentyl–POSS–DGEBA nanofillers in their effect on the DGEBA–D2000 thermomechanical properties. DMTA spectra: (1) DGEBA–D2000 reference; (2): 33 epoxy-mol % (25 wt %) cyclopentyl–POSS–DGEBA cured at 120 °C; (3) POSS nanocomposite additionally postcured at 180 °C for 12 h under argon; (4) POSS nanocomposite additionally postcured at 180 °C for 12 h in air; (5) 25 amino-mol % (24 wt %) Sn4 cured at 120 °C; (6) 25 mol % Sn4 additionally postcured at 180 °C under air; (a) $G' = f(T)$; (b) $\tan(\delta) = f(T)$.

nanoaggregation was observed via SAXS and TEM and plays a useful role in the mechanical matrix reinforcement.

The stannoxane dodecamers were shown to partly oligomerize (18%) during the epoxy network cure at 120 °C. At higher temperatures, the nanofiller oligomerization inside its domains becomes prominent. This process does not change the sample's overall morphology, and the thermo-mechanical properties remain practically unchanged. However, the oligomerization most likely contributes to the nanofiller's low extractability, which is a useful effect.

The ability of the stannoxane nanofiller to protect (via oxidative cross-linking) the epoxy matrix against the oxidative degradation of mechanical properties is a very attractive feature. For this purpose, already a few weight percent of stannoxane are sufficient. In this context, the difficult extractability of the stannoxane (stabilizer) is highly advantageous.

AUTHOR INFORMATION

Corresponding Author

*Telepnone: (+420) 296 809 384. E-mail: strachota@imc.cas.cz.

ACKNOWLEDGMENTS

The authors thank Ms. Miroslava Kremličková for carrying out the TGA experiments, Ms. Dana Kaňková for recording a large part of the NMR spectra, Ing. Magdalena Perchacz MSc. for taking part in the final stages of the synthesis work, and Ms. Zuzana Walterová and Ms. Zuzana Kálalová for the determination of the tin content via ash analysis.The authors thank the Grant Agency of the Academy of Sciences of the Czech Republic, Grant Nr. IAA400500701, the European Community's Human Potential Program under Contract

HPRN-CT-2002−00306, and the Czech Science Foundation, Grant Nr. 108/11/2151 for the financial support of this work. The authors thank Huntsman Inc. for the donation of Jeffamine D2000.

REFERENCES

(1) Miri, V.; Elkoun, S.; Peurton, F.; Vanmansart, C.; Lefebvre, J. M.; Krawczak, P.; Seguela, R. *Macromolecules* **2008**, *41*, 9234−9244.
(2) Treece, M. A.; Oberhauser, J. P. *Macromolecules* **2007**, *40*, 571−582.
(3) Lee, Y. H.; Bur, A. J.; Roth, S. C.; Start, P. R. *Macromolecules* **2005**, *38*, 3828−3837.
(4) Durmus, A.; Ercan, N.; Soyubol, G.; Deligoz, H.; Kasgoz, A. *Polym. Compos.* **2010**, *31*, 1056−1066.
(5) Matteucci, S.; Van Wagner, E.; Freeman, B. D.; Swinnea, S.; Sakaguchi, T.; Masuda, T. *Macromolecules* **2007**, *40*, 3337−3347.
(6) Weng, C. J.; Huang, J. Y.; Huang, K. Y.; Jhuo, Y. S.; Tsai, M. H.; Yeh, J. M. *Electrochim. Acta* **2010**, *55*, 8430−8438.
(7) Tunc, S.; Duman, O. *LWT-Food Sci. Technol.* **2010**, *44*, 465−472.
(8) Rao, Y. Q.; Chen, S. *Macromolecules* **2008**, *41*, 4838−4844.
(9) Kuila, B. K.; Park, K.; Dai, L. M. *Macromolecules* **2010**, *43*, 6699−6705.
(10) Antonello, A.; Brusatin, G.; Guglielmi, M.; Martucci, A.; Bello, V.; Mattei, G.; Mazzoldi, P.; Pellegrini, G. *Thin Solid Films* **2010**, *518*, 6781−6786.
(11) Kim, H.; Abdala, A. A.; Macosko, C. W. *Macromolecules* **2010**, *43*, 6515−6530.
(12) Moniruzzaman, M.; Winey, K. I. *Macromolecules* **2006**, *39*, 5194−5205.
(13) Sahoo, S. K.; Kim, D. W.; Kumar, J.; Blumstein, A.; Cholli, A. L. *Macromolecules* **2003**, *36*, 2777−2784.
(14) Hammond, M. R.; Dietsch, H.; Pravaz, O.; Schurtenberger, P. *Macromolecules* **2010**, *43*, 8340−8343.
(15) Robbes, A. S.; Jestin, J.; Meneau, F.; Dalmas, F.; Sandre, O.; Perez, J.; Boue, F.; Cousin, F. *Macromolecules* **2010**, *43*, 5785−5796.
(16) Horak, D.; Trchova, M.; Benes, M. J.; Veverka, M.; Pollert, E. *Polymer* **2010**, *51*, 3116−3122.
(17) Horak, D.; Babic, M.; Jendelova, P.; Herynek, V.; Trchova, M.; Likavcanova, K.; Kapcalova, M.; Hajek, M.; Sykova, E. *J. Magn. Magn. Mater.* **2009**, *321*, 1539−1547.
(18) Priolo, M. A.; Gamboa, D.; Holder, K. M.; Grunlan, J. C. *Nano Lett.* **2010**, *10*, 4970−4974.
(19) Kim, H.; Macosko, C. W. *Macromolecules* **2008**, *41*, 3317−3327.
(20) Russo, G. M.; Simon, G. P.; Incarnato, L. *Macromolecules* **2006**, *39*, 3855−3864.
(21) Dong, W. F.; Liu, Y. Q.; Zhang, X. H.; Gao, J. M.; Huang, F.; Song, Z. H.; Tan, B. H.; Qiao, J. L. *Macromolecules* **2005**, *38*, 4551−4553.
(22) Matějka, L.; Strachota, A.; Pleštil, J.; Whelan, P.; Steinhart, M.; Šlouf, M. *Macromolecules* **2004**, *37*, 9449−9456.
(23) Strachota, A.; Kroutilová, I.; Kovářová, J.; Matějka, L. *Macromolecules* **2004**, *37*, 9457−9464.
(24) Strachota, A.; Whelan, P.; Kříž, J.; Brus, J.; Urbanová, M.; Šlouf, M.; Matějka, L. *Polymer* **2007**, *48*, 3041−3058.
(25) Brus, J.; Urbanova, M.; Strachota, A. *Macromolecules* **2008**, *41*, 372−386.
(26) Eychenne-Baron, C.; Ribot, F.; Steunou, N.; Sanchez, C. *Organometallics* **2000**, *19*, 1940−1949.
(27) Ribot, F.; Banse, F.; Diter, F.; Sanchez, C. *New J. Chem.* **1995**, *19*, 1145−1153.
(28) Ribot, F.; Lafuma, A.; Eychenne-Baron, C.; Sanchez, C. *Adv. Mater.* **2002**, *14*, 1496−1499.
(29) Ribot, F.; Veautier, D.; Guillaudeu, S. J.; Lalot, T. *J. Mater. Chem.* **2005**, *15*, 3973−3978.
(30) Ribot, F.; Escax, V.; Martins, J. C.; Biesemans, M.; Ghys, L.; Verbruggen, I.; Willem, R. *Chem.—Eur. J.* **2004**, *10*, 1747−1751.
(31) Van Lokeren, L.; Willem, R.; van der Beek, D.; Davidson, P.; Morris, G. A.; Ribot, F. *J. Phys. Chem. C* **2010**, *114*, 16087−16091.
(32) Weiss, R. A.; Yu, W. C. *Macromolecules* **2007**, *40*, 3640−3643.
(33) Osborn, S. J.; Hassan, M. K.; Divoux, G. M.; Rhoades, D. W.; Mauritz, K. A.; Moore, R. B. *Macromolecules* **2007**, *40*, 3886−3890.
(34) Shah, R. K.; Paul, D. R. *Macromolecules* **2006**, *39*, 3327−3336.
(35) Xu, L.; Weiss, R. A. *Macromolecules* **2003**, *36*, 9075−9084.
(36) Puff, H.; Reuter, H. *J. Organomet. Chem.* **1989**, *373*, 173−178.
(37) Dakternieks, D.; Zhu, H.; Tiekink, E. R. T.; Colton, R. J. *J. Organomet. Chem.* **1994**, *476*, 33−38.
(38) Chandrasekhar, V.; Gopal, K.; Singh, P.; Narayanan, R. S.; Duthie, A. *Organometallics* **2009**, *28*, 4593−4601.
(39) Holmes, R. R. *Acc. Chem. Res.* **1989**, *22*, 190−194.
(40) Ribot, F. In *Tin Chemistry: Fundamentals, Frontiers, and Applications*; Davies, A. G.. Gielen, M., Pannell, K. H., Tiekink, E. R. T., Eds. ; Wiley, Chichester (UK), 2008; pp 69−92.
(41) Eychenne-Baron, C.; Ribot, F.; Steunou, N.; Sanchez, C. *J. Organomet. Chem.* **1998**, *567*, 137−142.
(42) Matejka, L. *Macromolecules* **1989**, *22*, 2911−2917.
(43) Gilman, J. W.; Schlitzer, D. S.; Lichtenhan, J. D. *J. Appl. Polym. Sci.* **1996**, *60*, 591−596.
(44) Verker, R.; Grossman, E.; Eliaz, N. *Acta Mater.* **2009**, *57*, 1112−1119.
(45) Sarantopoulou, E.; Kollia, Z.; Cefalas, A. C.; Siokou, A. E.; Argitis, P.; Bellas, V.; Kobe, S. *J. Appl. Phys.* **2009**, *105*, 114305.